Title

Endothelial NOTCH1 is suppressed by circulating lipids and antagonizes inflammation during atherosclerosis

Journal

Journal of Experimental Medicine, 212(12)

ISSN

0022-1007

Authors

Briot, Anaïs
Civelek, Mete
Seki, Atsuko
et al.

Publication Date

2015-11-16

DOI

10.1084/jem.20150603

Peer reviewed

Endothelial NOTCH1 is suppressed by circulating lipids and antagonizes inflammation during atherosclerosis

Anaïs Briot,[1] Mete Civelek,[2] Atsuko Seki,[3] Karen Hoi,[1] Julia J. Mack,[1] Stephen D. Lee,[3,5] Jason Kim,[3,5] Cynthia Hong,[3,5] Jingjing Yu,[1] Gregory A. Fishbein,[3] Ladan Vakili,[2] Alan M. Fogelman,[2] Michael C. Fishbein,[3] Aldons J. Lusis,[2] Peter Tontonoz,[3,5] Mohamad Navab,[2] Judith A. Berliner,[2,3] and M. Luisa Iruela-Arispe[1,4]

[1]Department of Molecular, Cell, and Developmental Biology, [2]Department of Medicine, [3]Department of Pathology and Laboratory Medicine, David Geffen School of Medicine, and [4]Molecular Biology Institute, University of California, Los Angeles, Los Angeles, CA 90095
[5]Howard Hughes Medical Institute, Los Angeles, CA 90095

Although much progress has been made in identifying the mechanisms that trigger endothelial activation and inflammatory cell recruitment during atherosclerosis, less is known about the intrinsic pathways that counteract these events. Here we identified NOTCH1 as an antagonist of endothelial cell (EC) activation. NOTCH1 was constitutively expressed by adult arterial endothelium, but levels were significantly reduced by high-fat diet. Furthermore, treatment of human aortic ECs (HAECs) with inflammatory lipids (oxidized 1-palmitoyl-2-arachidonoyl-*sn*-glycero-3-phosphocholine [Ox-PAPC]) and proinflammatory cytokines (TNF and IL1β) decreased Notch1 expression and signaling in vitro through a mechanism that requires STAT3 activation. Reduction of NOTCH1 in HAECs by siRNA, in the absence of inflammatory lipids or cytokines, increased inflammatory molecules and binding of monocytes. Conversely, some of the effects mediated by Ox-PAPC were reversed by increased NOTCH1 signaling, suggesting a link between lipid-mediated inflammation and Notch1. Interestingly, reduction of *NOTCH1* by Ox-PAPC in HAECs was associated with a genetic variant previously correlated to high-density lipoprotein in a human genome-wide association study. Finally, endothelial Notch1 heterozygous mice showed higher diet-induced atherosclerosis. Based on these findings, we propose that reduction of endothelial NOTCH1 is a predisposing factor in the onset of vascular inflammation and initiation of atherosclerosis.

The Journal of Experimental Medicine

Maintenance of endothelial homeostasis is critical to the prevention of vascular disorders including hypertension, atherosclerosis, and thrombosis (Siti et al., 2015). Events that trigger these pathologies, particularly atherosclerosis, require endothelial activation frequently driven by proatherogenic molecules such as lipid oxidation products, TNF, and IL-1β (Brånén et al., 2004; Lee et al., 2012; Qamar and Rader, 2012). Oxidized 1-palmitoyl-2-arachidonoyl-*sn*-glycero-3-phosphocholine (Ox-PAPC) strongly activates atherogenic pathways in human aortic endothelial cells (ECs [HAECs]) and regulates the expression of more than 1,000 genes (Gargalovic et al., 2006). Involvement of this oxidized lipid product in atherogenic processes is corroborated by studies showing that antibodies to Ox-PAPC inhibit atherogenesis in mice and Ox-PAPC levels correlate with atherosclerosis in human studies (Lichtman et al., 2013). However, the specific mechanisms that sense atherogenic lipids and transduce these readouts into transcriptional changes are poorly understood.

Correspondence to M. Luisa Iruela-Arispe: arispe@mcdb.ucla.edu

Abbreviations used: EC, endothelial cell; GWAS, genome-wide association study; HAEC, human aortic EC; HDL, high-density lipoprotein; HFD, high-fat diet; NICD, Notch intracellular domain; Ox-PAPC, oxidized 1-palmitoyl-2-arachidonoyl-*sn*-glycero-3-phosphocholine; qRT-PCR, quantitative RT-PCR; SNP, single nucleotide polymorphism.

Notch signaling is a critical pathway in embryonic development of vertebrate and invertebrate organisms (Guruharsha et al., 2012). In the vascular system, all Notch receptors (Notch1–4) and ligands (Jag1 and 2 and Dll1, 3, and 4) are expressed, albeit at different levels and distinctly in different vascular cells and vessel types. Activation of Notch receptors requires binding to a transmembrane ligand presented by adjacent cells. In canonical Notch signaling, this binding enables a series of successive cleavage events in the receptor, ultimately resulting in the release of the intracellular region of NOTCH (Notch intracellular domain [NICD]). NICD, the transcriptionally active form of Notch, translocates to the nucleus where it regulates a broad range of target genes. Notch signaling is required during vascular development, specification, and remodeling of the vascular tree, and defects in this pathway result in several vascular disorders (Gridley, 2010; Rostama et al., 2014). Although the protein is expressed in mature arteries, the biological contributions of Notch in adult stable vessels are less understood. In general terms, Notch1 has been considered to promote endothelial quiescence, and its absence (or repression) is a requirement to

The Rockefeller University Press $30.00
J. Exp. Med. 2015 Vol. 212 No. 12 2147–2163
www.jem.org/cgi/doi/10.1084/jem.20150603

initiate sprouting angiogenesis (Hellström et al., 2007; Lobov et al., 2007; Suchting et al., 2007). However, its contributions in adult vessels in vivo are less clear and might reveal tissue-specific differences (Ramasamy et al., 2014).

In adult ECs, Notch1 and Notch4 have been shown to prevent apoptosis in a rat cardiac allograft model (MacKenzie et al., 2004; Quillard et al., 2008) and in response to laminar blood flow (Walshe et al., 2011; Rostama et al., 2014). Apoptosis contributes to the disruption of the intima, after injury or inflammatory events. Intriguingly, endothelial Notch signaling is affected by inflammatory conditions, and its down-regulation appears to correlate with an inflammatory status in the endothelium. For example, Notch4 in small coronary vessels is repressed by TNF, and this triggers an increase in Vcam1 at the cell surface (Quillard et al., 2008). In bone marrow ECs, the canonical Notch effector RBP-jk inhibits Mir-155 and NF-κB (Wang et al., 2014). In addition, loss of RBP-jk heterozygosity sensitizes mice to cardiac valve disease when fed a high-fat diet (HFD), through a process that included accumulation of monocytes in the valve leaflets and calcification (Nus et al., 2011). In both cases, deletion of the RBP-jk is expected to result in loss of Notch signaling. Recent work, using induced pluripotent stem cell (iPSC)–derived ECs in vitro, showed that *NOTCH1* haploinsufficiency disrupts the EC response to shear stress and unlocks pro-osteogenic and inflammatory networks (Theodoris et al., 2015). The emergence of an inflammatory network was intriguing and unexpected. Importantly, the biological significance of these findings remained to be explored in vivo.

In this study, we show that NOTCH1 is the main Notch receptor expressed in human adult arterial ECs and present evidence that endothelial Notch1 plays an important role in preventing inflammation in the aorta. We found that expression and activity of Notch1 was rapidly reduced by HFD in mouse endothelium and by exposure to proatherogenic factors (Ox-PAPC, TNF, and IL-1β) in HAECs. Notably, decrease of Notch1 signaling in the absence of any external stimuli promoted monocyte binding to ECs in vitro and in vivo and led to an increase in proinflammatory and atherogenic molecules (IL8, CXCL1, SELE, CHST1, and TDAG51), suggesting that Notch1 actively prevents the emergence of an inflammatory phenotype. We also found that retention of Notch1 signaling nullified some of the multiple effects mediated by Ox-PAPC in HAECs. Finally, we found that heterozygous endothelial-specific deletion of Notch1 in mice accelerated atherosclerosis. Collectively, our findings indicate that Notch1 signaling contributes to the stability and homeostasis of adult ECs and protects against vascular inflammation during the early phases of atherosclerosis.

RESULTS

NOTCH1 is constitutively expressed in the endothelium of adult arteries but shows variable levels across individuals

To assess the relative levels of Notch receptors in HAECs, we first compared transcripts for all Notch receptors by quantitative RT-PCR (qRT-PCR). Among the four members of the family, *NOTCH1* was the most prevalent (Fig. 1 A). At the protein level, NOTCH1 was sixfold higher in HAECs than in smooth muscle cells isolated from the human aorta (HASMCs; Fig. 1, B and C). Immunodetection of NOTCH1 in human coronary arteries further confirmed its expression in adult endothelium (Fig. 1 D, arrows) and also indicated conspicuous absence from vascular smooth muscle cells (Fig. 1 D). Additional measurements of NOTCH1 expression of 14 human coronary arteries from individuals lacking atheroma (NOTCH1 area/CD31 area) uncovered high variability across the specimens (ranging from 7 to 53%; Fig. 1 E). A broad range of expression of Notch1 in large vessel human endothelium was also confirmed by microarray analysis of HAECs isolated from 147 individuals (Fig. 1 F). Therefore, although NOTCH1 is abundant in the endothelium, levels appear to be variable across donors. We were intrigued by this variation and also by the unclear function of Notch1 in adult endothelium. Potential reasons for variability in Notch expression included age, gender, genetic modifiers, and/or epigenetic modifications imposed by predisposing conditions such as diabetes, hyperlipidemia (diet), etc. Evaluation of gender and age provided no insight. Thus, we turned our attention to other factors.

Notch1 expression and signaling is suppressed by exposure to an HFD in mice

The initial stages of atherosclerosis are characterized by activation and disruption of the endothelial barrier, events that are induced in mice by hyperlipidemia. We next inquired whether hyperlipidemia was a reason behind the variability observed in NOTCH1 expression in vivo. HFD (Fig. 2 A) in mice induced a rapid increase in plasma cholesterol levels (Fig. 2 B). Transcriptional analysis of aortic ECs from these mice fed for 4–13 d revealed that a proatherogenic diet was able to significantly decrease *Notch1* and its canonical target gene: *Hey1* (Fig. 2 C). Restoration of normal plasma cholesterol levels (4 d HFD followed by 3 d chow; Fig. 2 B) rescued Notch1 signaling (as per *Notch1* and *Hey1* levels; Fig. 2 C), supporting a direct impact of circulating lipids on Notch1. In addition, we found that endothelial *Notch1* and *Hey1* mRNA levels were inversely correlated with circulating cholesterol levels at early time points (Fig. 2 D). These data revealed that hyperlipidemia negatively affects Notch1 signaling in adult endothelium in mice. Next, we inquired whether this was also true for human cells, particularly in relation to oxidized (proatherogenic) lipids and cytokines.

Oxidized phospholipids, TNF, and IL-1β repress NOTCH1 in human ECs

Hyperlipidemia and increased levels of inflammatory cytokines are hallmarks of atherosclerosis; we thus tested whether proatherogenic mediators such as oxidized lipids, TNF, and IL-1β could affect NOTCH1 in human ECs. Using HAECs, we found that levels of *NOTCH1*, as well as the target genes

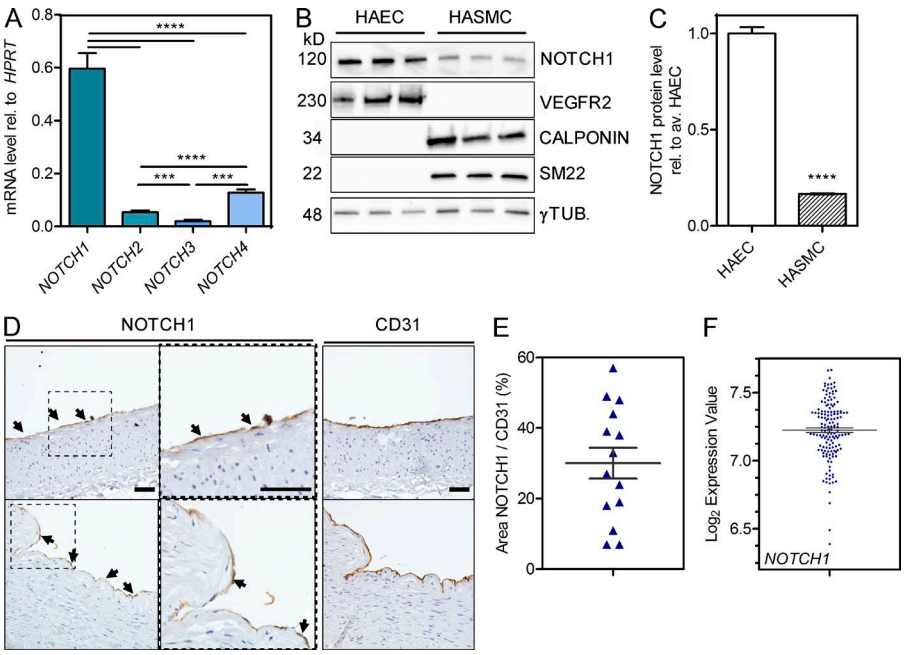

Figure 1. **NOTCH1 is constitutively expressed by adult arterial endothelium.** (A) Relative levels of Notch receptors measured by qRT-PCR in HAECs (n = 11; three donors). (B and C) Western blot performed on cultured HAECs (n = 3 donors; VEGFR2 positive) and HASMCs (n = 3 donors; SM22 and Calponin positive). Relative protein level was measured by densitometry and normalized to loading control γ-Tubulin (γTUB). Mean values detected in HAECs are used as the reference point (value = 1), and data are presented as mean ± SEM. ****, $P < 0.0001$; ***, $P < 0.001$ by paired (A) and unpaired (C) Student's t test. (D) Immunohistochemistry performed on human coronary arteries from normal individuals. NOTCH1 was detected in the endothelium (left and middle; arrows), which was also positive for CD31 (right). Dotted box panels (middle; NOTCH1 staining) are higher magnifications of the dotted areas presented in the adjacent left panels. Bars, 50 µm. (E) Quantification of area covered by NOTCH1 in human coronary arteries from vessels without atherosclerosis (n = 14 sections) on a linear region of 500 µm in length. (F) *NOTCH1* transcript levels from 147 HAECs isolated from independent individual heart transplant donors were measured by microarray analysis and represented as Log2 expression values. Data are represented as mean ± SEM.

HES1 and *HEYL*, were reduced by all three stimuli. Although *JAG1* was up-regulated upon cytokine treatment, its expression was repressed by Ox-PAPC (Fig. 3, A and B). This suggested that some components of Notch signaling are differentially modulated by inflammatory cytokines versus Ox-PAPC; both common and divergent mechanisms are likely involved in Notch regulation by the two types of stimuli.

To uncover possible common mechanisms that could explain how two distinct effectors (TNF and Ox-PAPC) mediate NOTCH1 suppression, we evaluated a large group of pharmacological inhibitors. Particularly, we asked whether specific inhibitors could revert the ability of TNF and/or Ox-PAPC to suppress *NOTCH1* and *HES1*. From the inhibitors examined, blockade of STAT3 (Stattic) abolished the transcriptional repression of *NOTCH1* and *HES1* by TNF or Ox-PAPC (Fig. 3, C and D). Importantly, even in the absence of external stimuli, inhibition of STAT3 increased basal levels of *NOTCH1* and *HES1* (Fig. 3, C and D). These data highlighted a unifying process for the suppression of NOTCH1 downstream two distinct, athero-promoting effectors (TNF or Ox-PAPC) in HAECs.

To assess the reproducibility and biological impact of Ox-PAPC on *NOTCH1*, we took advantage of our previously published microarray experiments that include assessment of cultured HAECs from 147 individual donors (Romanoski et al., 2010). 40 µg/ml Ox-PAPC suppressed *NOTCH1* expression in 80% of the donors after 4 h of treatment (Fig. 3 E). In addition, time course analysis confirmed that NOTCH1 protein was significantly affected after Ox-PAPC treatment and that the repression was maintained over time (Fig. 3, F and G).

A more comprehensive evaluation indicated that although the response was variable between individuals, *NOTCH1* was always decreased between 6 and 8 h after Ox-PAPC exposure (Fig. 3, H–J). Furthermore, the Notch ligand *JAG1* and target genes *HES1* and *HEYL* were rapidly and irreversibly decreased upon Ox-PAPC exposure (Fig. 3, J and K).

The variability of *NOTCH1* at basal conditions, as well as the level and kinetics of down-regulation by Ox-PAPC treatment suggested that genetic variants contribute to the regulation of *NOTCH1* by Ox-PAPC. Information from single nucleotide polymorphisms (SNPs) obtained from the 147 donors was used to seek further clarification. We assessed which variants were involved in the response of *NOTCH1* to Ox-PAPC by using a genome-wide association study (GWAS) focusing on the level of *NOTCH1* down-regulation in response to Ox-PAPC as a quantitative trait. These experiments identified a suggestive peak on chromosome 11 (Fig. 3 L). The most significantly associated SNP (rs2923084) has also been shown to be associated with high-density

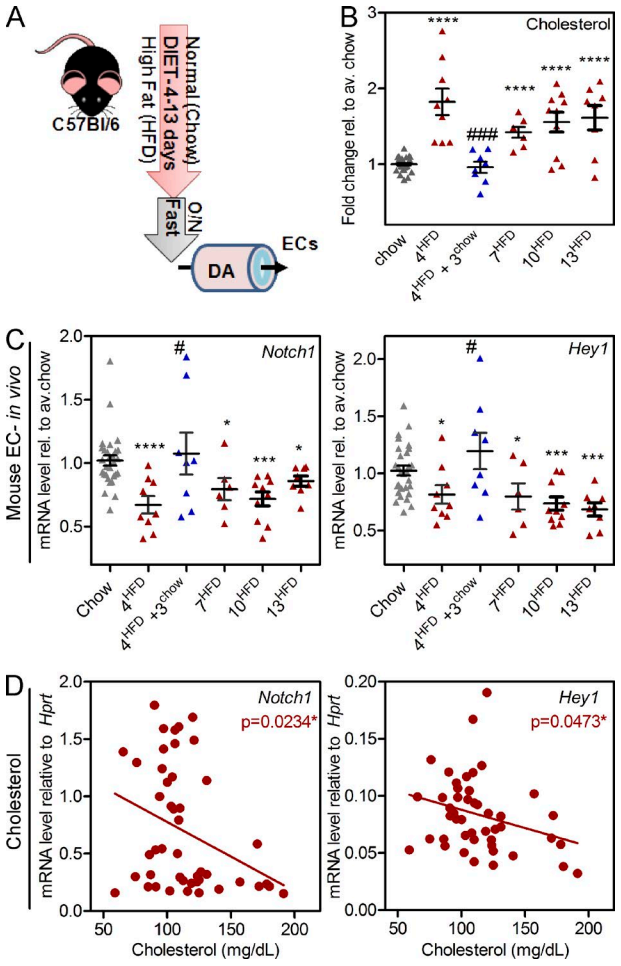

Figure 2. **Notch signaling is repressed by proatherogenic stimuli in vivo.** (A and B) C57BL/6J wild-type mice were fed a standard diet (chow) or HFD for 4–13 d or 4 d followed by a 3-d chow diet. After an overnight fast (A) circulating cholesterol levels were measured (B). The data are represented as fold change compared with the mean chow (B). (C) ECs were isolated from the descending aorta, and qRT-PCR was performed to determine *Notch1* and *Hey1* levels under HFD compared with chow. (B and C) Chow $n = 29$ and HFD $n = 6$–10. (D) Correlations between circulating cholesterol levels and endothelial mRNA levels of *Notch1* and *Hey1* at early time points ($n = 47$). ****, $P < 0.0001$; ***, $P < 0.001$; *, $P < 0.05$ relative to Chow; ###, $P < 0.001$; #, $P < 0.05$ relative to 4HFD, by unpaired Student's *t* test. Data are represented as mean ± SEM.

lipoprotein (HDL) levels in a human GWAS of ∼100,000 individuals (Teslovich et al., 2010; Willer et al., 2013). The SNP is located in a noncoding RNA (CAD11.1) whose function in ECs has not been studied. The nearest protein coding genes are *AMPD3* (*adenosine monophosphate deaminase 3*) and *ADM* (*Adrenomedullin*); however, the expression level of neither of these genes is associated with rs2923084. The G allele of the SNP was determined to be the risk allele linked with lower HDL levels in humans compared with the A allele. We found that the individuals with the G allele displayed greater decrease in *NOTCH1* transcript in response to Ox-PAPC (Fig. 3 M), suggesting that the genetic variant regulating HDL levels has an effect on the response of *NOTCH1* to Ox-PAPC in ECs. Together with the observation that *Notch1* levels were correlated with circulating cholesterol in mice (Fig. 2), these data on primary human cells support the notion that endothelial NOTCH1 levels and activity are modulated by hyperlipidemia.

Repression of NOTCH1 alone results in activation of a common subset of Ox-PAPC targets

To investigate the biological relevance of Notch1 suppression in early atherogenic events triggered by inflammatory phospholipids, we compared the transcript profile of HAEC knockdown for *NOTCH1* with profiles from HAECs treated with Ox-PAPC (Fig. 4). Gene microarray analysis revealed that ∼14% of the transcripts regulated by Ox-PAPC were also regulated in the same direction when NOTCH1 was reduced (Fig. 4 A). Validation by qRT-PCR performed on the same samples showed that Heme oxygenase (*HMOX-1*) was increased by Ox-PAPC and siRNA-mediated knockdown of *NOTCH1* (Fig. 4, B and C). In addition, we observed that suppression of NOTCH1 led to an increase in IL-8 and CXCL1 at the mRNA and protein levels (Fig. 4, C–E). These are two powerful chemokines that favor recruitment of leukocytes to the endothelium during atherosclerosis. These proinflammatory mediators were also consistently overexpressed in the 147 donors after 4 h of Ox-PAPC treatment (Fig. 4, F and G). Noticeably, whereas overexpression of *IL8* was rapid and sustained over time, *CXCL1* up-regulation showed an early and transient response to Ox-PAPC (Fig. 4, I and J). Moreover, Ox-PAPC treatment and down-regulation of NOTCH1 led to a significant increase in the endoplasmic reticulum stress factor *TDAG51* (Fig. 4, B–D), which has been described to favor atherosclerosis (Hossain et al., 2003). Although *TDAG51* levels showed high variability across donors at 4 h after Ox-PAPC treatment (Fig. 4 H), a time course analysis revealed that this increase can occur at early time points and transiently in some individuals (Fig. 4 K). Finally, we also observed some differences. Knockdown of *NOTCH1* led to an increase in *SELE* (encoding CD62E/E-Selectin) and *CHST1* (Li et al., 2001), a protein involved in leukocyte rolling; this increase was not observed when HAECs were exposed to Ox-PAPC (Fig. 4, B–D).

Suppression of NOTCH1 by Ox-PAPC participates in downstream proatherogenic effects

The shared transcriptional profile between Ox-PAPC and NOTCH1 suppression suggested that repression of Notch1 signaling may be a prerequisite for some of the effects mediated by Ox-PAPC. To test this possibility, we evaluated the effect of Notch1 retention in the presence of Ox-PAPC.

We first transduced HAECs with lentiviral particles expressing the intracellular domain of rat *Notch1* that included the γ-secretase cleavage-dependent region (ZEDN1 [Shawber et al., 1996]). This form enables overexpression,

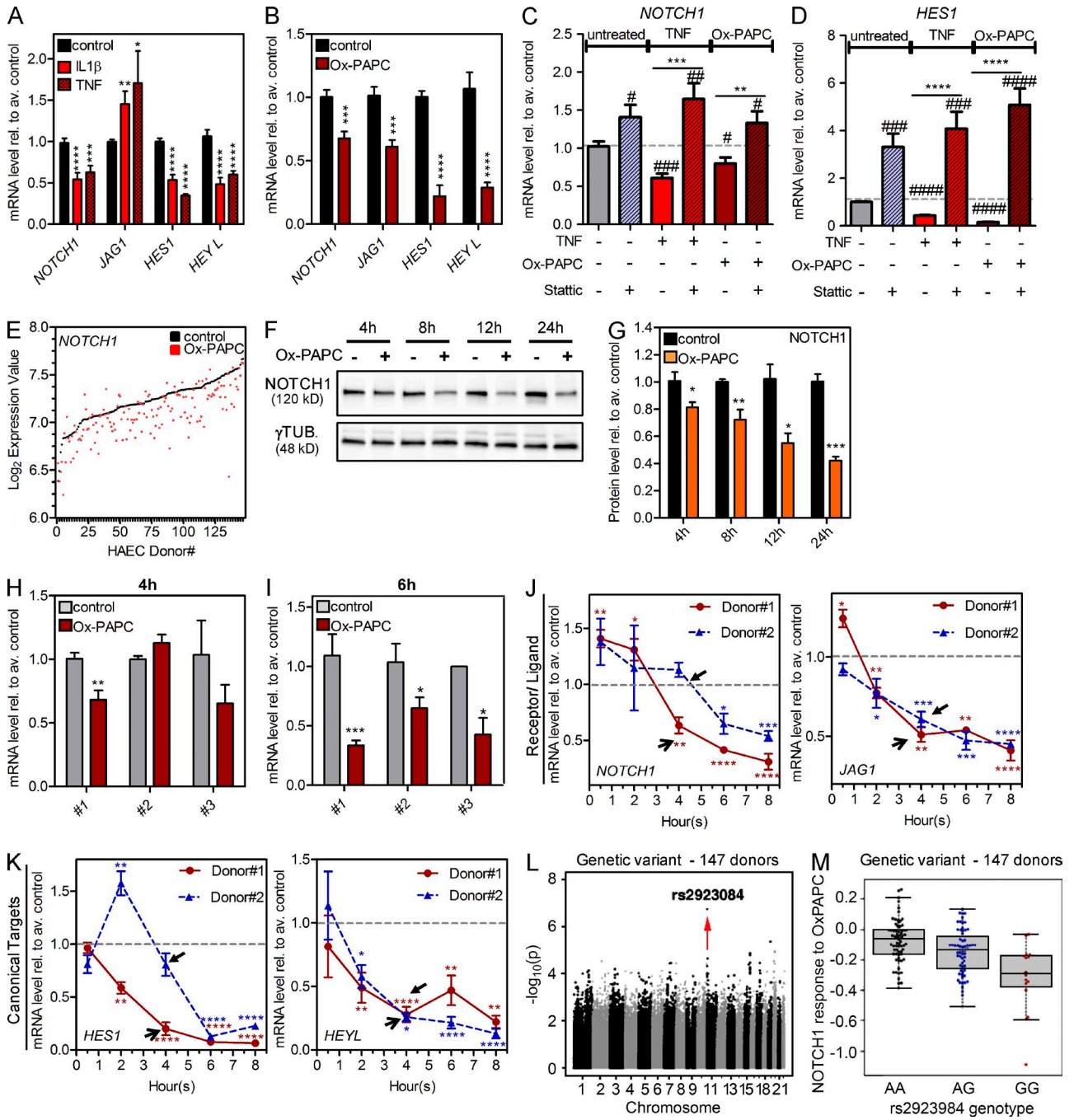

Figure 3. **Inflammatory cytokines and Ox-PAPC repress NOTCH1 expression and signaling in HAECs.** (A and B) HAECs were treated with recombinant 10 ng/ml IL1β, 10 ng/ml TNF, or 50 µg/ml Ox-PAPC for 4 h. Transcript levels of Notch signaling molecules were measured by qRT-PCR (n = 6–15; three donors). (C and D) HAECs were treated with 10 ng/ml TNF or 50 µg/ml Ox-PAPC for 4 h in the presence of STAT3 inhibitor (10 µM Stattic) or vehicle control (n = 8–14; four to five donors); mRNAs level of *NOTCH1* and *HES1* were measured by qRT-PCR. (E) Microarray analysis of *NOTCH1* levels in 147 HAECs isolated from individual donors untreated (black dots) or treated with 40 µg/ml Ox-PAPC (red dots) for 4 h are shown and represented as Log2 expression values. (F–K) HAECs were treated with 50 µg/ml Ox-PAPC for the indicated times. (F and G) NOTCH1 protein was detected by Western blot, and relative amount was measured by densitometry and normalized by γ-TUBULIN (γTUB; n = 3 donors). (H and I) *NOTCH1* mRNA level at 4 and 6 h after treatment with Ox-PAPC in three independent donors (#1–3). (J and K) Transcript levels of *NOTCH1*, *JAG1*, *HES1*, and *HEYL* were measured over time after Ox-PAPC treatment by qRT-PCR (n = 4; two donors). Bottom (Donor#1) and top (Donor#2) arrows indicate the differences in the regulation of target genes after 4 h of treatment. Data are represented as mean ± SEM. ****, P < 0.0001; ***, P < 0.001; **, P < 0.01; *, P < 0.05 by unpaired Student's t test. In C and D, $^{\#\#\#\#}$, P < 0.0001; $^{\#\#\#}$, P < 0.001; $^{\#\#}$, P < 0.01; $^{\#}$, P < 0.05 to control-treated cells by unpaired Student's t test. (L and M) Degrees of *NOTCH1* repression after treatment with Ox-PAPC were mapped to SNPs across the genome using data from 147 donors. The Manhattan plot shows the significance of association at each SNP marker across the genome. The red arrow shows the peak SNP of association (L). Boxplots of the change in *NOTCH1* expression in each donor are shown based on the genotype of the peak association SNP (M).

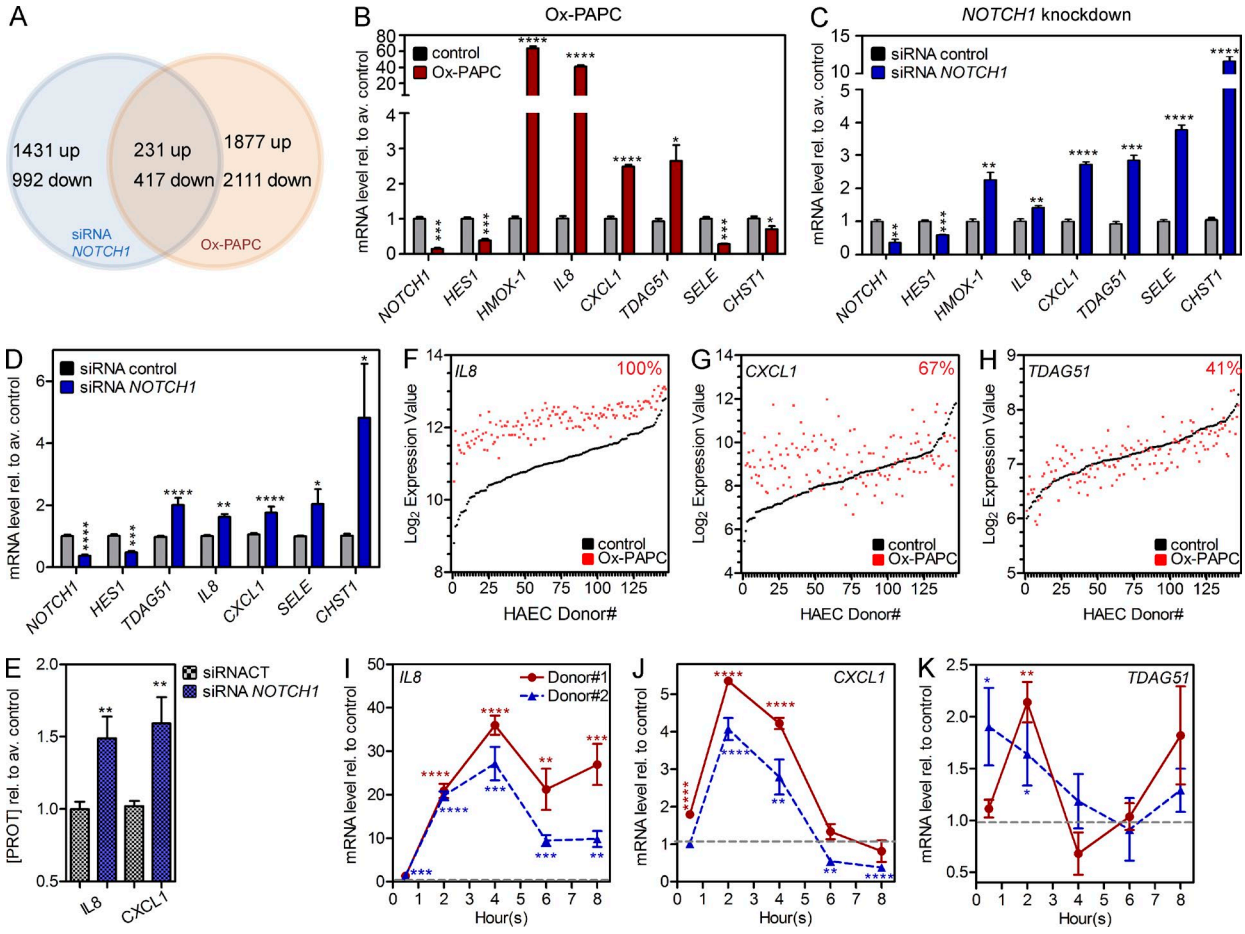

Figure 4. **Knockdown of *NOTCH1* shares transcriptional targets with Ox-PAPC.** (A–C) The transcriptional profile of HAECs treated with siRNA *NOTCH1* or 50 µg/ml Ox-PAPC (6 h) was analyzed by gene microarray. (A) Venn diagram indicating overlapping and independent transcripts changed by Ox-PAPC or knockdown of *NOTCH1*. (B and C) Validation by qRT-PCR analyses ($n = 3$ each condition). (D) *IL8*, *CXCL1*, *TDAG51*, *SELE*, and *CHST1* were measured by qRT-PCR in additional HAEC donors treated with siRNA control or targeting *NOTCH1* ($n = 9–11$). (E) IL8 and CXCL1 protein levels were measured by ELISA in the culture supernatant of HAECs treated with siRNA control or targeting *NOTCH1* ($n = 6$; three donors). (F–H) HAECs from 147 heart transplant donors were treated (red dots) or not (black dots) with 40 µg/ml Ox-PAPC (4 h). mRNA levels of *IL8* (F), *CXCL1* (G), and *TDAG51* (H) were measured by gene microarray analysis and represented as Log2 expression values. The percentage of donors with increased level of the interest transcript under Ox-PAPC treatment is indicated on each graph in red. (I–K) HAECs were treated for the indicated time with 50 µg/ml Ox-PAPC. Levels of *IL8*, *CXCL1*, and *TDGA51* were measured by qRT-PCR ($n = 4$; two donors). ****, $P < 0.0001$; ***, $P < 0.001$; **, $P < 0.01$; *, $P < 0.05$ by unpaired Student's *t* test. Data are represented as mean ± SEM.

but it retains some level of physiological regulatory control through enzymatic processing (Fig. 5 A). ZEDN1 includes the transmembrane domain of Notch1, and thus it is anchored until the γ-secretase complex releases the intracellular domain of the receptor (NICD; in S3; Fig. 5 A). This is important because we and others found that overexpression of the unbound cytoplasmic fragment NICD (independent of γ-secretase complex activity) is toxic and results in senescence and apoptosis (Liu et al., 2012). Using the membrane-retaining construct, we confirmed that rat *Notch1* was present only in the cells infected with lentivirus-expressing ZEDN1 but was absent in HAECs transduced with control lentivirus (Fig. 5 B). ZEDN1 was also detected by protein analysis at the anticipated molecular weight (Fig. 5 C, red arrow) and below the endogenous p120-S1 (Fig. 5 C, black arrow). To reduce potential off-target effects caused by supraphysiological expression, we performed all of the evaluations using the lowest possible dose of ZEDN1 (Fig. 5 C). HAECs transduced with ZEDN1 in the absence of Ox-PAPC showed a slight but significant decrease in *TDAG51* transcript, whereas *JAG1* and *HEYL* were clearly increased, confirming that the transgene was active on canonical Notch targets. No changes were observed in *IL8*, *CXCL1*, and *HES1* (Fig. 5 D) in the absence of Ox-PAPC treatment. Expression of ZEDN1 in the presence of Ox-PAPC rescued *JAG1*, *HES1*, and *HEYL* transcripts, indicating that Notch1 activity was retained, even under circumstances when endogenous human *NOTCH1* was suppressed (Fig. 5 E). Maintenance of Notch1 signaling was also associated with a partial but significant (50%) rescue

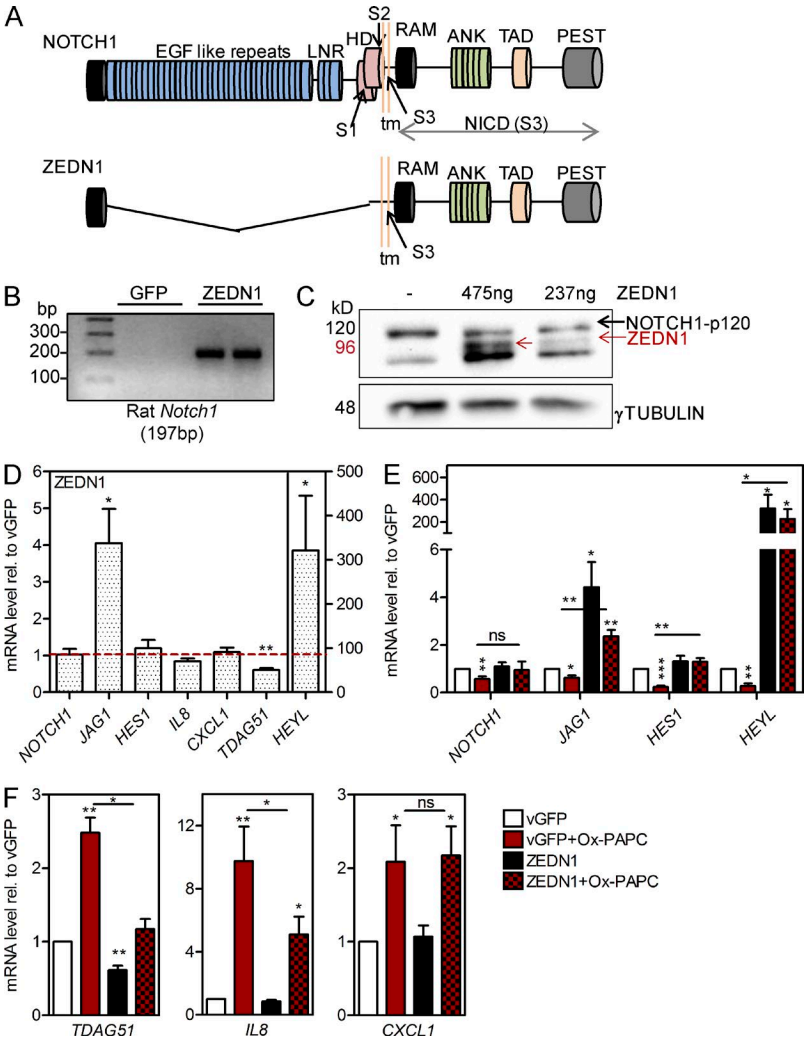

Figure 5. **Maintenance of NOTCH1 signaling rescues the induction of *TDAG51* and *IL8* by Ox-PAPC.** (A) Schema of ZEDN1 (rat NICD bound to the plasma membrane) construct that was cloned in a CMV-GFP lentiviral vector. S1–3, proteolytic cleavage sites; LNR, Lin12/Notch repeats; HD, heterodimerization domain; RAM, RBP-jk–associated molecule; ANK, ankyrin repeats; TAD, transactivation domain; PEST, proline, glutamate, serine, threonine rich. (B) Transcript of rat *Notch1* was detected by RT-PCR in HAECs transduced with lenti-ZEDN1. (C) Detection of endogenous NOTCH1-p120 (S1; black arrow) and ZEDN1 (red arrow) protein was detected in HAECs transduced with lenti-ZEDN1 by Western blot and normalized to γ-TUBULIN. (D) After transduction with lenti-ZEDN1 or GFP, *NOTCH1*, *JAG1*, *HES1*, *IL8*, *CXCL1*, *TDAG51*, and *HEYL* mRNA expression was measured by qRT-PCR. (E and F) HAECs were transduced with lentivirus encoding ZEDN1 or virus control (vGFP) and treated with 50 µg/ml Ox-PAPC (6 h) or control media. Notch signaling molecules (E) and downstream proatherogenic target (F) mRNA levels were determined by qRT-PCR. (D–F) $n = 5–6$; four donors. Data are represented as mean ± SEM. ***, $P < 0.001$; **, $P < 0.01$; *, $P < 0.05$ by paired Student's *t* test.

of *IL8* levels, whereas the effect of Ox-PAPC on *TDAG51* was completely abolished in the presence of ZEDN1. In contrast, regulation of *CXCL1* by Notch1 and Ox-PAPC appeared to occur through an alternative pathway, as retention of Notch1 signaling did not affect its up-regulation by Ox-PAPC (Fig. 5 F). Thus, in HAECs, repression of NOTCH1 appears to mediate some of the effects of Ox-PAPC (for *IL8* and *TDAG51*), but it also affects gene expression through independent mechanisms (for *CXCL1*).

Decrease in NOTCH1 promotes binding of leukocytes to ECs in vitro and in vivo

Our data demonstrated that NOTCH1 reduction impacted expression of proinflammatory and proatherogenic molecules (Fig. 4). These events are predicted to facilitate recruitment and binding of leukocytes to the endothelium. Therefore, we reduced the expression of *NOTCH1* in confluent HAEC monolayers with siRNA (Fig. 6 A) and performed leukocyte adherence assays with labeled THP-1 monocytes. Decrease of NOTCH1 in the confluent monolayer of HAECs in the absence of external stimuli led to a significant increase in monocyte binding (Fig. 6, B and C). Similarly, CD45 immunodetection in endothelial-specific heterozygous deletion of Notch1 (VeCad-Cre^{+}, Notch1$^{F/+}$; N1$^{EC+/-}$) revealed an enhanced binding and subendothelial infiltration of immune cells compared with wild-type mice (N1^{ECWT}; Fig. 6 D). In accordance with our in vitro data on HAECs (Fig. 4), partial reduction of Notch1 in ECs in vivo resulted in increased CXCL1 detection in the endothelium of N1$^{EC+/-}$ animals when compared with wild type (Fig. 6 E).

To further assess the biological consequence of loss of Notch1 in the mature aorta, we induced its deletion from the endothelium of adult mice (Cdh5-Cre^{ERT2} Notch1$^{F/F}$; N1^{ECKO}). These animals also expressed Cre-inducible Tomato reporter, allowing for visualization of recombined cells. En face fluorescence imaging revealed single and multiple leukocytes bound to the endothelium of N1^{ECKO} aortae (Fig. 6, G–J, arrows). These findings further support the notion that Notch1 is constantly required to maintain a quiescent status and prevent EC activation and inflammation in the aorta.

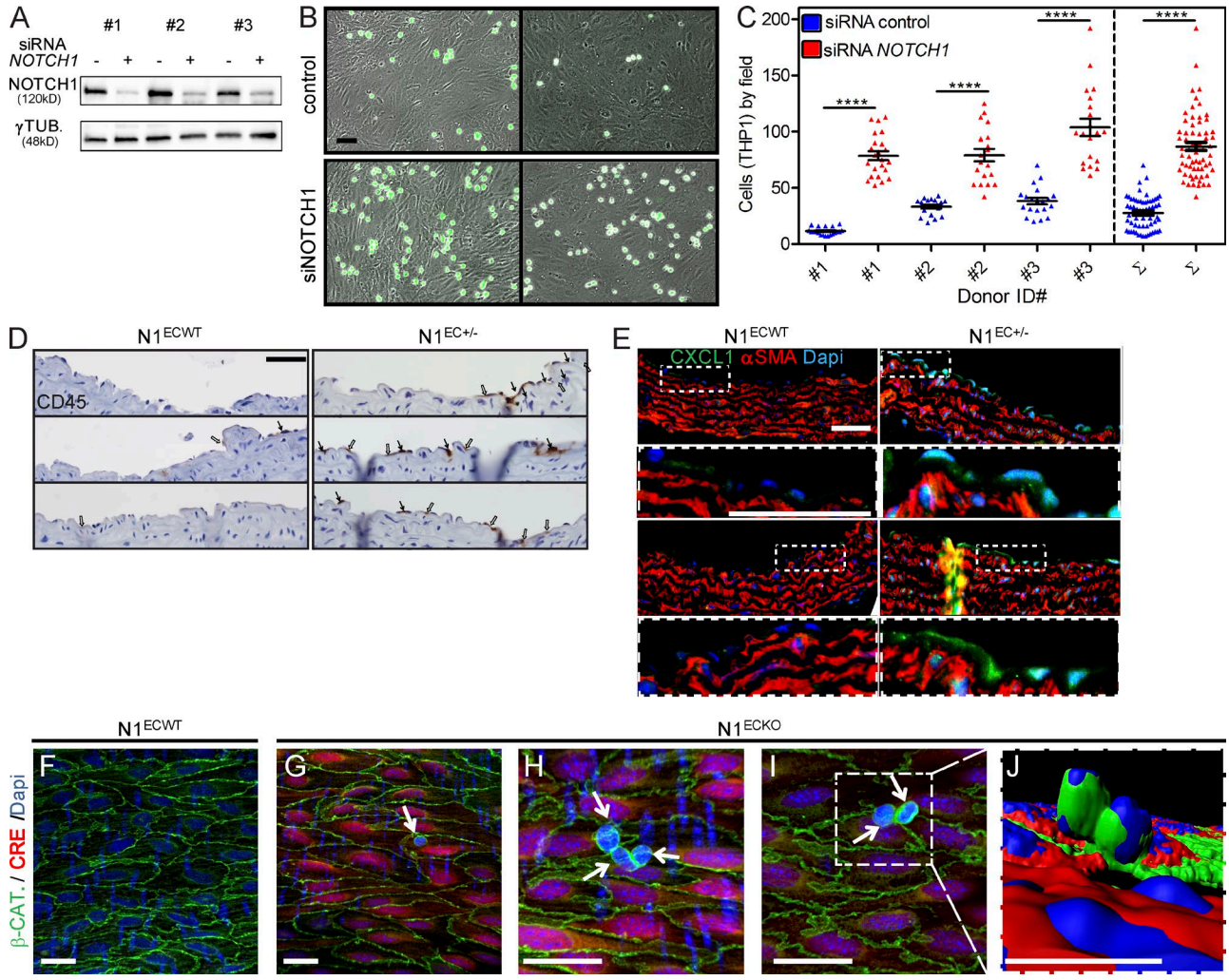

Figure 6. **Decrease in endothelial *NOTCH1* expression increases monocyte binding in vitro and in vivo.** (A) NOTCH1 protein level was evaluated in HAECs transfected with control siRNA or siRNA targeting *NOTCH1*. γ-TUBULIN (γTUB) was used as a loading control. (B and C) The confluent monolayers of HAECs were then cocultured with CFSE-labeled THP-1 monocytes. CFSE-labeled THP-1 (green, B) bound to the monolayer was counted in 10 fields per donor and condition (n = 6; three donors). Σ indicates data from the three donors grouped. ****, P < 0.0001 by unpaired Student's t test. Mean ± SEM is shown. (D) $CD45^{POS}$ leukocytes were detected by immunohistochemistry on aortic sections from $N1^{ECWT}$ and $N1^{EC+/-}$ mice. Black arrows, $CD45^{POS}$ cells at the surface of the endothelium; open arrows, $CD45^{POS}$ cells underneath the endothelium. (E) Co-immunostaining of CXCL1/GRO-α and αSMA was performed on aortic sections from $N1^{ECWT}$ and $N1^{EC+/-}$ mice. Lower dotted box panels are higher magnifications of the dotted boxes in the panels above. (D and E) Six to nine animals per genotype were examined; representative sections are shown. (F–J) 5-wk-old Notch1-floxed or $Cdh5\text{-}Cre^{ERT2}$–negative ($N1^{ECWT}$; n = 4) or –positive ($N1^{ECKO}$; n = 5) littermates were injected with tamoxifen to induce Notch1 deletion in the endothelium. Descending aortae were harvested 2 wk later, stained for β-Catenin to define cell junctions (green), and used for en face confocal imaging. Recombined, Notch1 knockout, ECs were positive for Tomato reporter (red, G–J). Tomato-negative leukocytes were detected at the endothelium surface of $N1^{ECKO}$ animals (arrows; G–J). (J) 3D reconstitution of I. Bars: (B) 50 µm; (D and E) 25 µm; (F–J) 20 µm. (E–J) Nuclei were stained with Dapi.

Hemizygous deletion of endothelial Notch1 increases predisposition to atherosclerosis in L-sIDOL mice

Given the previous findings, we speculated that repression of Notch1 might contribute to the onset of atherosclerosis through regulation of EC activation. To test this hypothesis, we crossed mice with specific heterozygous EC-Notch1 ($N1^{EC+/-}$) to a diet-induced atherosclerosis model expressing a liver-specific dominant-active form of IDOL (L-sIDOL; Fig. 7 A; Calkin et al., 2014).

Adult $N1^{EC+/-}$ mice, maintained on a standard diet, showed significantly higher numbers of $CD45^{POS}$ cells in the aortic arch when compared with the $N1^{ECWT}$/L-sIDOL. Similarly, hemizygous deletion of *Notch1* in the L-sIDOL background ($N1^{EC+/-}$/L-sIDOL) led to increased accumulation of inflammatory cells (Fig. 7, B and C). In addition, we observed that CXCL1 was enhanced in the endothelium of the mice lacking one allele of endothelial Notch1 when compared with L-sIDOL animals (Fig. 7 D).

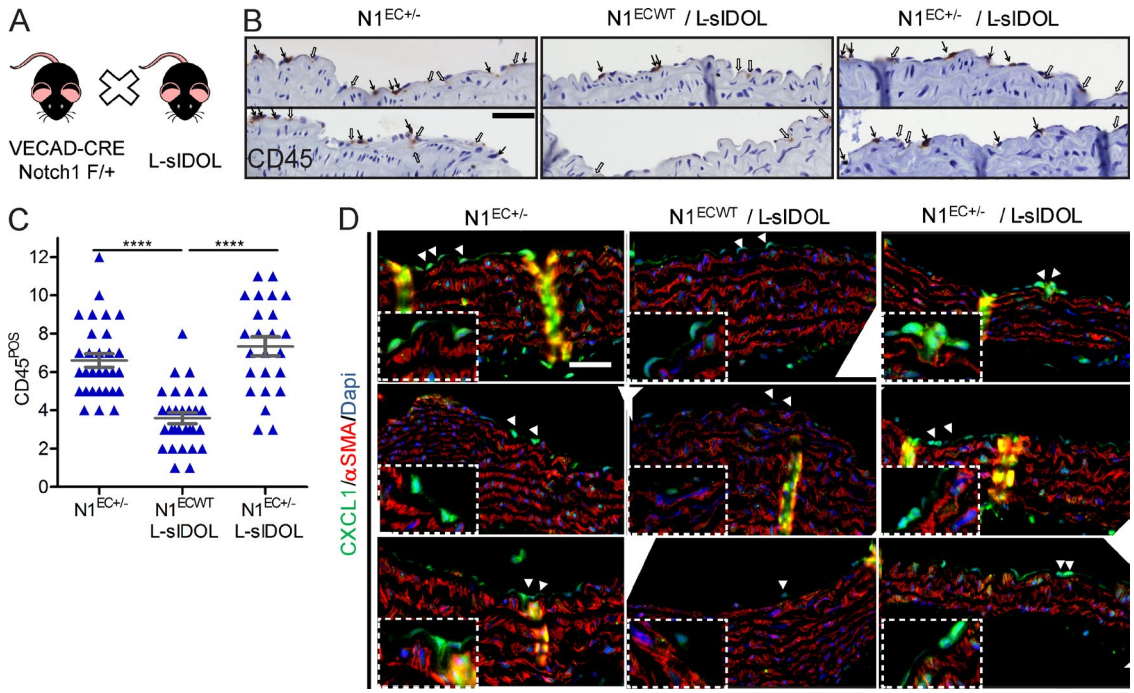

Figure 7. **Decrease in endothelial Notch1 increases basal inflammation in L-sIDOL animals.** (A) Mice with heterozygous deletion of *Notch1* in the endothelium $N1^{EC+/-}$ were crossed with transgenic L-sIDOL mice ($N1^{EC+/-}$/L-sIDOL). (B and C) $CD45^{POS}$ leukocytes were detected by immunohistochemistry on aortic sections from $N1^{EC+/-}$, $N1^{ECWT}$/L-sIDOL, and $N1^{EC+/-}$/L-sIDOL animals. Black arrows, $CD45^{POS}$ cells at the surface of the endothelium; open arrows, $CD45^{POS}$ cells underneath the endothelium. Quantification of accumulated $CD45^{POS}$ cells was assessed per 280-µm endothelium length in aortic cross section from adult animals. ****, $P < 0.0001$ by unpaired Student's *t* test. Mean ± SEM is shown. (D) Co-immunostaining of CXCL1/GRO-α and αSMA was performed on aortic sections from $N1^{EC+/-}$, $N1^{ECWT}$/L-sIDOL, and $N1^{EC+/-}$/L-sIDOL animals. Dotted box panels are higher magnifications of the cells indicated by arrowheads in each panel. Nuclei are stained with Dapi. Cross sections from 9–10 animals per genotype were examined; representative sections are shown. Bars, 25 µm.

To assess the contribution of decreased endothelial Notch1 to atherosclerosis, 6-wk-old mice ($N1^{EC+/-}$, $N1^{ECWT}$/L-sIDOL, and $N1^{EC+/-}$/L-sIDOL) were fed a normal (chow) or HFD for 28 wk. Regardless of their genotypes, HFD resulted in elevated levels in plasma cholesterol (Fig. 8 A). No Sudan IV–positive lesions were observed in mice fed a chow diet (Fig. 8, B and D). When fed an HFD, small lesions were detected in the descending aorta and femoral arteries of $N1^{EC+/-}$ animals (Fig. 8, C and E). Transgenic mice on HFD developed early atherosclerosis; however, $N1^{EC+/-}$/L-sIDOL animals showed a significant increase in en face aorta lesions when compared with the $N1^{ECWT}$/L-sIDOL (3.58-fold; Fig. 8, C and E; and Table 1). Aortic root lesion size followed the same trend with an increased mean surface in the $N1^{EC+/-}$/L-sIDOL compared with the $N1^{ECWT}$/L-sIDOL (2.81-fold; Table 1). We also observed extended lesions that invaded the arch branches in $N1^{EC+/-}$/L-sIDOL (Fig. 8 E). Together, these findings indicate that hemizygous loss of Notch1 in the endothelial compartment increases susceptibility to atherosclerosis. Altogether, these data indicate that suppression of NOTCH1 in the endothelium may contribute to the onset of atherosclerosis by de-repressing inflammatory and atherogenic molecules (IL-8, CXCL1, and TDAG51).

DISCUSSION

In this study we showed that constant basal Notch1 signaling protects against EC activation in large vessels. We observed that atherogenic stimuli rapidly repressed Notch1 in vitro and in vivo. Furthermore, reduction in endothelial Notch1, even in the absence of external stimuli triggers endothelial activation, increased leukocyte binding, and overexpression of proatherogenic molecules. Importantly, data presented here also showed that Notch1 levels are affected by circulating lipids. Finally, this study demonstrates that Notch1 reduction in the endothelium increases diet-induced atherosclerosis. Additional evidence for a role of Notch signaling in atherosclerosis was provided recently by two integrative genomic studies that examined GWAS results for coronary artery disease. These studies evaluated data-driven tissue-specific gene networks (Mäkinen et al., 2014) and Reactome pathways (Ghosh et al., 2015) and identified genetic signals to be enriched in NOTCH pathway genes. In accordance with these findings, our data provide a link between endothelial Notch1 regulation and atherosclerosis and reveal mechanisms responsible for this outcome.

The role of Notch signaling in atherosclerosis has been previously studied in human and mouse models but yielded

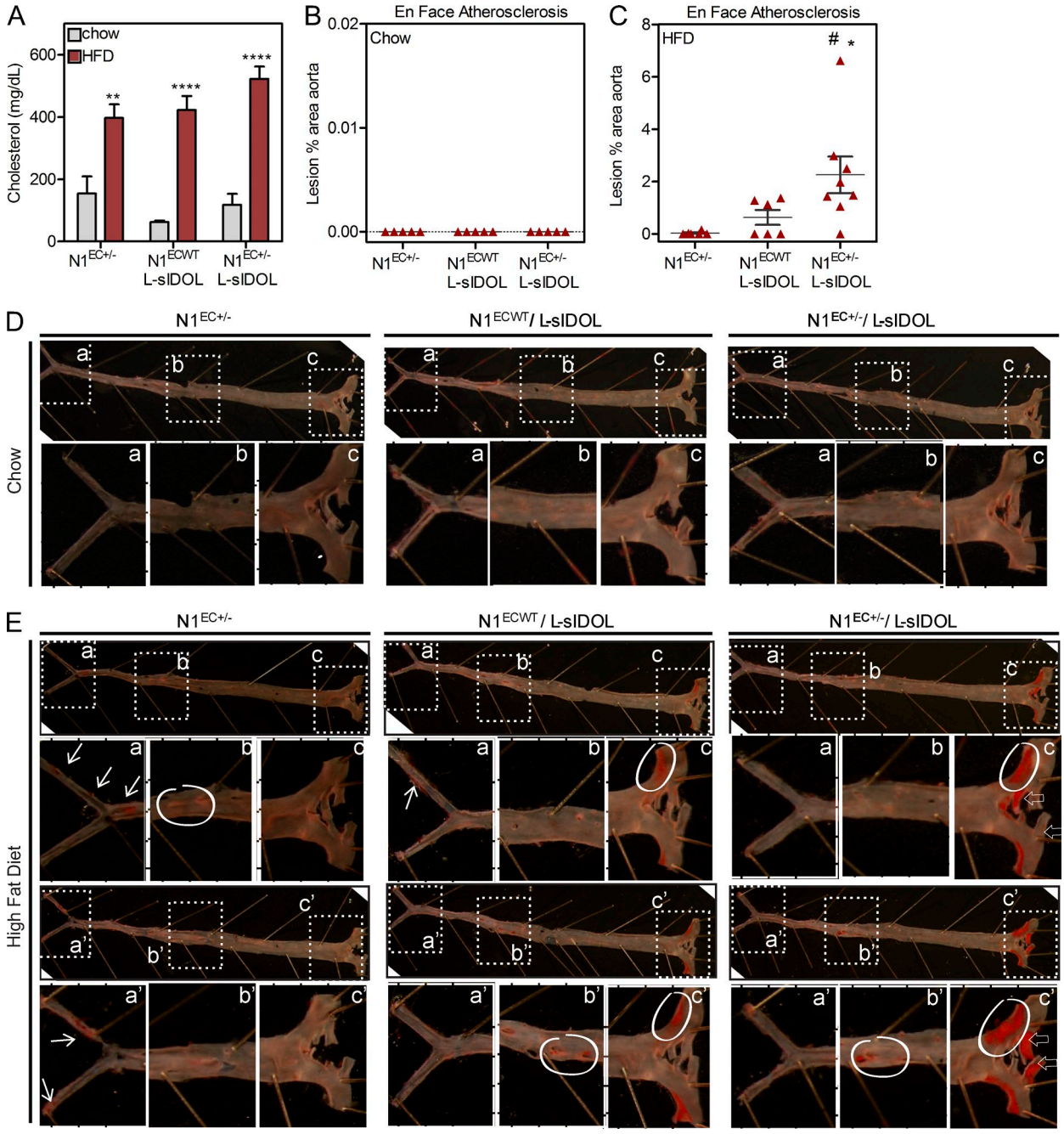

Figure 8. **Hemizygous loss of endothelial Notch1 increases diet-induced atherosclerosis in L-sIDOL mice.** 6-wk-old mice with heterozygous deletion of *Notch1* in the endothelium were crossed with transgenic L-sIDOL mice ($N1^{EC+/-}$/L-sIDOL) and fed for 28 wk a standard diet (chow) or HFD. (A) Plasma cholesterol was measured after 28 wk on chow or HFD. (B–E) En face aorta atherosclerosis was assessed by Sudan IV staining to detect the subintimal accumulation of lipids. Mean ± SEM are shown (A–C). In the $N1^{EC+/-}$ animals, lesions were observed in the descending aorta (b, ellipsis) and femoral arteries (a and a′, white arrows; E); in the $N1^{EC+/+}$/L-sIDOL and $N1^{EC+/-}$/L-sIDOL animals, lesions were also found in the aortic arch (c and c′, ellipses; E) and the arch branches (open arrows; E). (A) ****, $P < 0.0001$; **, $P < 0.01$ by unpaired Student's *t* test. (C) #, $P = 0.011$ relative to $N1^{EC+/-}$; *, $P = 0.038$ by Mann–Whitney test relative to $N1^{EC+/+}$/L-sIDOL. Animals fed chow, $n = 5$ per genotype; HFD, $N1^{EC+/-}$ and $N1^{EC+/+}$/L-sIDOL $n = 6$ and $N1^{EC+/-}$/L-sIDOL $n = 8$.

contradictory conclusions (Quillard et al., 2008, 2010; Aoyama et al., 2009; Nus et al., 2011; Fukuda et al., 2012; Liu et al., 2012; Rizzo et al., 2013; Schober et al., 2014). Administration of γ-secretase inhibitors, and therefore blockade of global Notch signaling, was associated with a decrease in diet-induced plaque burden in $ApoE^{-/-}$ mice. This effect

Table 1. **Atherosclerosis measurement in N1/L-sIDOL mice**

Genotype	En face	Root
	%	μm^2/section
$N1^{ECWT}$/L-sIDOL	0.630 ± 0.28	11,229 ± 3,304
$N1^{EC+/-}$/L-sIDOL	2.254 ± 0.70	31,555 ± 10,511
Fold change	3.58 ± 1.111	2.81 ± 0.936

Fold change indicates $N1^{EC+/-}$/L-sIDOL over $N1^{ECWT}$/L-sIDOL. Data are presented as mean ± SEM.

was attributed to a reduction of Notch activity in $MOMA2^+$ macrophages (Aoyama et al., 2009). Although relevant when considering a systemic blockade of the disease, γ-secretase inhibitors are broad spectrum and impact several enzymatic pathways, signaling molecules, and receptors (De Strooper, 2003). Other studies have also found that administration of antibodies to the ligand Dll4 attenuates atherosclerosis. Once again the mechanism was linked to an effect on macrophages (Fukuda et al., 2012). Conversely, other studies have proposed a protective role for Notch signaling in several vascular diseases. Nus et al. (2011) showed that mice with global haploinsufficiency of the Notch pathway effector RBP-jk developed diet-induced calcific aortic valve disease with accumulation of macrophages and collagen deposition. A protective role for Notch signaling has also been supported by a study of Notch2 and Notch4 on ECs (Quillard et al., 2010) of small coronary vessels in rats with heart transplants (Quillard et al., 2008). There, the authors observed that decrease in Notch4 impaired vascular repair after transplantation in vivo and proposed a role for Notch signaling in the maintenance of EC quiescence. They also proposed that Notch was required for optimal survival and repair in response to injury. More recently, it was demonstrated that endothelial Mir-126 was antiinflammatory and essential for the maintenance of a proliferative pool of progenitor ECs in the aorta. Administration of this microRNA to mice limited atherosclerosis via the repression of the Notch antagonist Dlk1, once again implying an inhibitory role for Notch signaling in atherosclerosis (Schober et al., 2014).

In the present work, we provide evidence that NOTCH1 is the most predominant Notch receptor in arterial ECs of human and mouse (Fig. 1; Briot et al., 2014). We also showed that Notch1 is a key regulator of arterial EC homeostasis and that it functions as a sensory link between circulating lipids and atherosclerosis susceptibility. We observed that suppression of Notch1 in the absence of external stimuli leads to overexpression of major proinflammatory and atherogenic mediators (IL8, CXCL1, SELE, and TDAG51) and increased binding of leukocytes in vitro and in vivo. In accordance with previous studies, it is undeniable that partial loss of Notch1 has a broad impact on the EC transcriptome. Theodoris et al. (2015) showed that heterozygous mutation of NOTCH1 in iPSC-derived ECs altered the transcriptional regulation of multiple genes, with predominant signatures in osteogenic and inflammatory genes.

Table 2. **Transcription factors predicted to regulate shared target genes of Ox-PAPC and NOTCH1 knockdown in HAECs**

Factor	Genes	Q-value
Sin3a	536	1.17×10^{-22}
Corest	375	3.78×10^{-12}
P300	414	4.38×10^{-10}
Hdac2	290	2.35×10^{-9}
Hdac1	240	7.39×10^{-4}
Ctbp2	85	2.49×10^{-2}
Irf1	193	6.96×10^{-13}
Irf3	69	1.26×10^{-3}
Irf4	121	4.43×10^{-6}
Cebpb	374	4.88×10^{-10}
Cebpd	227	1.22×10^{-9}
Nfkb	364	4.01×10^{-12}
Stat1	42	1.52×10^{-3}
Stat2	43	1.39×10^{-10}
Stat3	93	6.44×10^{-5}
Egr1	460	8.54×10^{-13}
Creb1	360	5.26×10^{-11}
Atf1	179	1.19×10^{-6}
Atf2	192	3.59×10^{-4}
Atf3	243	1.03×10^{-5}
Srebp1	89	2.45×10^{-4}
Tal1	110	7.00×10^{-4}

A subset of transcription factors predicted to regulate genes changed by 25%, 1% FDR by 50 µg/ml Ox-PAPC (6 h), and NOTCH1 knockdown are shown. The Genes column shows the number of genes in our list that are regulated by the indicated transcription factor.

Similarly, using siRNA, we found a large cohort of transcription factors altered when NOTCH1 was reduced in adult HAECs. Many of these factors are known to regulate the inflammatory response (such as STAT, NF-κB, CEBP, and EGR1). Interestingly, some of these genes are known to be activated in response to Ox-PAPC treatment (CREB, SREBP, ATF3, and STAT3; Lee et al., 2012). We also noted changes in cofactors involved in NOTCH signaling and chromatin modification (SIN3, HDAC, CoREST, and p300; Table 2). Thus, repression of Notch1 in arterial endothelium results in profound transcriptional and functional changes, leading to proinflammatory states.

Among its proinflammatory targets, NOTCH1 knockdown in HAECs led to a significant increase in CXCL1 expression. Accumulation of CXCL1 on the luminal side of the endothelium has been shown to promote monocyte recruitment in $ApoE^{-/-}$ mice that was blocked by injection of antibodies targeting the cytokine (Zhou et al., 2011). Thus, the intrinsic increase of CXCL1 observed in HAECs with knockdown of *NOTCH1* and in the endothelium of $N1^{EC+/-}$ mice indicates that this transcription factor could be protective during the early phases of atherosclerosis. This notion was further supported by our observation that hemizygous loss of Notch1 in the endothelium ($N1^{EC+/-}$) increased diet-induced atherosclerosis in the L-sIDOL background. Thus, we propose that the intrinsic endothelial activation state of the $N1^{EC+/-}$/L-sIDOL aggravates their sensitivity to the development of atherosclerosis.

Our data provide evidence for the role of oxidized lipids and cytokines associated with atherosclerosis in the regulation of endothelial Notch1. Indeed, in vitro TNF as well as atherogenic doses of Ox-PAPC rapidly repress NOTCH1 through a Stat3-dependent mechanism. Importantly, both Ox-PAPC and TNF were previously shown to activate STAT3 (Guo et al., 1998; Lee et al., 2012); therefore, this appears to be a unifying mechanism that results in *NOTCH1* suppression by distinct effectors.

It is important to highlight, however, that Ox-PAPC and suppression of Notch1 (by siRNA) are not identical in the regulation of all inflammatory genes. For example, although Notch1 suppression increases E-Selectin and CHST1 Ox-PAPC does not. This might be at first counterintuitive because Ox-PAPC induces Notch1 repression. However, Ox-PAPC is composed of several active oxidized phospholipids such as 1-Palmitoyl-2-(5-oxovaleroyl)-*sn*-glycero-3-phosphorylcholine (POVPC) and 1-palmitoyl-2-glutaroyl-*sn*-glycero-3-phosphorylcholine (PGPC; Watson et al., 1997). These subproducts have been shown to selectively activate distinct pathways. In particular, it has been shown that although POVPC represses the induction of E-Selectin by LPS, PGPC induces its expression (Leitinger et al., 1999). Thus, this apparent competing effect of Ox-PAPC active subproducts may account for the differences observed between "simple" reduction of NOTCH1 by siRNA and treatment with Ox-PAPC.

Although the effect of lipid products in vitro and long-term HFD have been shown to impact the endothelium transcriptome (Lee et al., 2012; Erbilgin et al., 2013b), we show that transcriptional repression of Notch1 signaling molecules in vivo occurs as early as 4 d after starting an HFD. This effect was reversible, as switching from HFD to normal diet rescued Notch1 signaling, demonstrating a link between diet and endothelial Notch1 signaling. The unexpected regulation of Notch1 by circulating lipids was also supported by additional evidence from mice and human studies. In fact, we observed a negative correlation between circulating cholesterol levels and transcriptional expression of *Notch1* in vivo. Human genetic experiments showed a significant association between a genetic variant on chromosome 11 with *NOTCH1* responses to Ox-PAPC in HAECs (Fig. 3, L and M). This variant was previously associated with HDL levels in a human GWAS (Teslovich et al., 2010). In fact, the G allele of this polymorphism was associated with a greater decrease of *NOTCH1* under Ox-PAPC stimulus (our data, Fig. 3 M) and a lower level of HDL in the previous study compared with the A allele (Teslovich et al., 2010). These data indicate that genetic variants that modulate *NOTCH1* (as per our study with 147 endothelial donors) are playing an important role in the effect of lipids on atherosclerosis.

The protective role of HDL against oxidation of lipids, the effect of oxidized lipids on the endothelium, and subsequent onset of atherosclerosis (Mineo and Shaul, 2013; Riwanto and Landmesser, 2013; Emert et al., 2014; Rye and Barter, 2014) reinforces the concept that low levels of NOTCH1 constitute an important predisposing and permissive factor to endothelial activation and atherosclerosis. In addition, the data presented here offer a link between diet and endothelial changes, leading to the acquisition of a proinflammatory status that precedes development of the disease. In this regard, Notch1 could be considered as a signaling hub that antagonizes the transduction of proatherogenic stimuli, thus preventing endothelial activation.

MATERIALS AND METHODS

Immunostaining and histological analysis. Tissue sections were deparaffinized, and antigen retrieval was performed with boiling citrate buffer (10 mM in PBS, pH 6) for detection of NOTCH1, CD45, αSMA, and CXCL1. Dako S1700 solution was used for detection of CD31. The source of the primary antibodies used include NOTCH1 and CD31 human (Cell Signaling Technology), αSMA and β-Catenin (Sigma-Aldrich), CXCL1/GROA (Abcam), and CD45 (BD). Imaging was performed with a BX40 light microscope (Olympus) or LSM 710 multiphoton confocal microscope (Carl Zeiss) using Zen software (Carl Zeiss). 3D reconstruction was generated using Imaris software (Bitplane).

We retrospectively reviewed microscopic slides of coronary arteries from 16 patients who received a heart transplant at the University of California, Los Angeles (UCLA), from 2008 to 2013. Tissues that underwent decalcification were excluded from the study (5 patients) because of poor immunohistochemical staining. In some cases, more than one cross section was used from a single coronary. Tissues were fixed with neutral-buffered formalin and embedded in paraffin, and 4-µm serial sections were taken. Staining of the serial sections was performed as described in the previous paragraph using EDTA, pH 8, antigen retrieval. Counter staining with hematoxylin was not performed on the slides stained with CD31 and NOTCH1 to optimize visualization. For image analysis, slides stained for NOTCH1 and CD31 were scanned with a digital slide scanner at 20× (Aperio XT scanner; Aperio Technologies). Randomly chosen relatively linear regions of endothelium (500 µm in length) were manually circled, and the circled areas were examined by Tissue Studio software (Definiens Inc.) to calculate the area positive for NOTCH1 and CD31. The same endothelial regions were carefully circled on NOTCH1 and CD31 slides from each tissue. For the visual analysis, we compared NOTCH1 and CD31 staining. Two observers examined these images. The study was approved by the Institutional Review Board (IRB) at UCLA (IRB#12-000608).

For atherosclerosis measurement, aortae were dissected, fixed (4% PFA, 5% sucrose, and 20 µM EDTA), and stained with Sudan IV. Images were captured with a CCD camera (DXC-97MD 3; Sony). Atherosclerosis in the aortic roots and the descending aortas (en face) were quantified by computer-assisted image analysis as described previously (Tangirala et al., 1995, 1999; Shih et al., 1998). Atherosclerotic lesions at the aortic valve were stained with Oil Red O and analyzed as described

previously (Shih et al., 1998). Lesion development is expressed as the percentage of total aortic surface covered by lesions (Bradley et al., 2007). Measurement of the lesions was performed by blinded investigator (mouse genotype and diet unknown).

Cells and Ox-PAPC treatment. HAECs were isolated from aortic explants of heart transplant donors in association with the UCLA Transplant Program. Isolation of HAECs involves selective enzymatic digestion and results in high purity of the ECs as previously described (Navab et al., 1988; Romanoski et al., 2011). Confluent HAECs in Medium 199 (Corning) supplemented with 1% heat-inactivated fetal bovine serum and 1% antibiotics were treated with Ox-PAPC as described in a previous publication (Romanoski et al., 2010), 10 ng/ml recombinant human TNF, or 10 ng/ml IL-1β. The dose of Ox-PAPC (40–50 μg/ml) used for these experiments was chosen based on experiments from our laboratory and others showing consistent atherogenic effects at this concentration (Lee et al., 2012). Although Ox-PAPC can have antiinflammatory action on bacterial products at much lower concentrations (Oskolkova et al., 2010), aortic extracts of oxidized phospholipid at the concentration used in this study have been shown to have proinflammatory effects on ECs (Subbanagounder et al., 2000; Oskolkova et al., 2010). For rescue experiments, confluent HAECs were pretreated with 10 μM Stattic (Selleck Chemicals) or vehicle control for 30 min; the cells were then treated with control media or media containing 10 ng/ml TNF or 40 μg/ml Ox-PAPC in the presence or not of the inhibitor for 4 h.

Mice. C57BL/6 mice were fed an HFD (#TD88137; Harlan Laboratories, Inc.) for the indicated time and fasted overnight before blood and tissue collection. For rescue experiments, mice were fed an HFD for 4 d and then switched to a standard diet for an additional 3 d.

Endothelial Notch1 heterozygous ($N1^{EC+/-}$) mice were crossed with L-sIDOL mice. 6-wk-old males were fed standard chow or an HFD (#D09062501R; Research Diet Inc.) for 28 wk. Mice were fasted overnight before euthanasia. VeCad-Cre/Notch1-floxed mice and L-sIDOL were previously described (Hofmann et al., 2012; Calkin et al., 2014).

For inducible endothelial deletion of Notch1, mice expressing floxed alleles of Notch1 (Radtke et al., 1999) were crossed to Cdh5(PAC)-CreERT2 transgenic animals (Wang et al., 2010) and mice expressing tdTomato reporter (Madisen et al., 2010). 5-wk-old mice received intraperitoneal injections of tamoxifen (1 mg/mouse; MP Biomedicals) for three consecutive days. After 2 wk, the animals were injected with methacholine chloride (6.5 mg/mouse; MP Biomedicals) in PBS and euthanized. Injection of methacholine chloride 2 min before euthanasia induces vascular smooth muscle relaxation and allows for en face imaging of the aorta. Aortae were harvested and fixed in 2% PFA before staining and mounting for en face confocal imaging. Mouse experiments were conducted in accordance with UCLA Department of Laboratory Animal Medicine's Animal Research Committee guidelines.

Blood parameters. Total mouse serum cholesterol and triglyceride were measured using Pointe Scientific Reagent Set (#C7509 and #T7531, respectively; Pointe Scientific). Data are represented as mean ± SEM.

Transcription analysis. Endothelial RNA-enriched fractions from mouse aortae were prepared as described previously (Briot et al., 2014). Total RNA from HAECs was purified using the RNeasy Mini kit (QIAGEN). Complementary DNA synthesis was performed with Superscript III reverse transcription First-Strand synthesis kit (Invitrogen) using oligo-dT primers.

qRT-PCR was performed using primers designed for human targets, provided in Table S1. Primers for mouse targets have been described previously (Briot et al., 2014). Each reaction was run in duplicate and normalized with *HPRT* housekeeping gene. P-values were calculated using the appropriate Student's *t* test. Data are represented as mean ± SEM. For gene microarray analysis, only RNA samples with RNA integrity numbers (RIN) of 7.0 or higher were used for subsequent processing.

Gene expression profiling analysis. The microarray results used for the analysis were described previously (Romanoski et al., 2010). Confluent cells from 147 donors were treated in duplicate with either control media or 40 μg/ml Ox-PAPC for 4 h. mRNA expression profiles from four samples per donor (two control treated and two Ox-PAPC treated) meeting quality control conditions were determined using the HT HG-U133A microarray (Affymetrix), which contains 18,630 probes. Intensity values were normalized with the robust multiarray average normalization method implemented in the *affy* package in Bioconductor (Gautier et al., 2004).

For expression profiling after siRNA-mediated *NOTCH1* silencing, HAECs transfected with siRNA targeting NOTCH1 or scrambled siRNA in the presence or absence of 50 μg/ml Ox-PAPC (6 h) in triplicate were used. Total RNA was hybridized to human HT-12 v4 Expression BeadChips (Illumina). Genome Studio software (2010.v3) was used for determination of probe fluorescence intensities. HT-12 BeadChip contains 48,804 expression and 786 control probes. The probes were processed using nonparametric background correction followed by quantile normalization with both control and expression probes used by the *neqc* function in the *limma* package (R v2.13.0; Ritchie et al., 2007). 20,202 probes with detection p-values <0.01 in any of the samples were applied for any further analysis. Differential gene expression analyses to compare cells transfected with siRNA against NOTCH1 or scrambled siRNA and cells treated with Ox-PAPC or cells transfected with scrambled siRNA was performed using the *limma* package in R (v2.13.0). Calculated p-values from the moderated Student's *t* statistics were adjusted using the Benjamini-Hochberg method for multiple testing. Microarray probes with adjusted values

of $P < 0.01$ (1% FDR) and fold change >25% were considered differentially expressed. The dataset for the gene microarray analysis on HAECs treated with *NOTCH1* siRNA or Ox-PAPC was deposited in the National Center for Biotechnology Information Gene Expression Omnibus database under accession no. GSE72633.

Genotyping and association analysis. Association of the SNPs and endothelial gene expression was described previously (Erbilgin et al., 2013a). In brief, HAEC genomic DNA was isolated using the DNeasy kit (QIAGEN). SNP genotyping was performed using the SNP 6.0 microarray platform (Affymetrix) as described previously (Romanoski et al., 2010). Microarray images were processed using the Genotyping Console 4.1 (Affymetrix) to make the SNP calls. SNPs were filtered out based on the following criteria: 296,063 SNPs with minor allele frequency <10%; 18,030 SNPs with <95% genotyping rate among the donors; 13,213 SNPs were set to missing because they were detected as heterozygous in haploid genotypes; and 3,890 SNPs were excluded because they failed the Hardy-Weinberg equilibrium test ($P < 10^{-4}$). A mixed model approach to account for the population structure as implemented in the EMMAX program was used to perform the association analysis (Kang et al., 2010).

We applied the linear mixed model

$$y = \mu + x\beta + u + e,$$

where μ = mean, x = SNP, β = SNP effect, and u = random effects caused by genetic relatedness, with $Var(u) = \sigma_g^2 K$ and $Var(e) = \sigma_e^2$, where K = IBS (identity by state) matrix across all genotypes in the panel. We computed a restricted maximum likelihood estimate for σ_g^2 and σ_e^2, and we performed association based on the estimated variance component with an F test to test β does not equal 0. The association analysis of SNPs with the difference in the expression value of the microarray probe set for NOTCH1 between Ox-PAPC treatment and control conditions was performed using the 574,391 informative SNPs that passed the filtering criteria. 108 males and 39 females were present in the donor population; therefore, sex was considered as a covariate in the mixed model for association analysis.

Western blot analysis. Cells were lysed in modified RIPA buffer containing 1% Triton X-100 and 10% SDS. Protein lysate were resolved and analyzed by Western blot using the following primary antibodies: NOTCH1 and VEGFR2 (Cell Signaling Technology), SM22 (Santa Cruz Biotechnology, Inc.), and Calponin and γ-Tubulin (Abcam). Quantification of bands by densitometry analysis was performed using ImageLab Software (Bio-Rad Laboratories).

siRNA-mediated knockdown. HAECs were transfected with stealth RNAi targeting *NOTCH1* (NM_017617.3_Stealth_775) or control duplexes (Invitrogen) using siPORT Amine (Ambion) as the transfection agent. For better efficiency, the cells were transfected twice with 24 h of recovery in between; cultures were then used for experiments 24 h after the second transfection.

ELISA. IL-8 and CXCL1/GROα levels in HAEC culture supernatants were measured with IL-8 and CXCL1 Quantikine ELISA kit (R&D Systems) according to the manufacturer's recommendation.

ZEDN1 lentivirus production and transduction. Lentivirus-based vectors encoding ZEDN1 (Shawber et al., 1996) and GFP genes were generated by transient cotransfection of 293T cells with a three-plasmid combination, as described previously (Naldini et al., 1996). In brief, 100-mm dishes of nonconfluent 293T cells were cotransfected with 6.5 μg pMDLg/pRRE, 3.5 μg pMDG (encoding the VSV-G envelope), 2.5 μg pRSV–REV, and 10 μg pRRL-CMV-ZEDN1-Ires-GFP by the CaPi-DNA coprecipitation method (Chen and Okayama, 1987; Sakoda et al., 1992). The following day, the medium was adjusted at a final concentration of 10 mM sodium butyrate, and the cells were incubated for 5 h to obtain high-titer virus production as previously described (Sakoda et al., 1999). After 5 h, cells were washed and incubated in fresh medium without sodium butyrate. Conditioned media was harvested the next day and passed through 0.45-mm filters. Viral titer was determined by assessing viral p24 antigen concentration by ELISA (the Alliance HIV-I p24 ELI SA kit) and hereafter expressed as micrograms of p24 equivalent units per milliliter.

HAECs at 50% confluency were transduced overnight with an equal amount of lentivirus expressing ZEDN1 (Shawber et al., 1996) or GFP control in the presence of 4 μg/ml protamine sulfate. Cells were allowed to recover and express the construct for an additional 48 h before experimentation. Primers designed to detect rat *Notch1* are forward, 5′-CAACTCTCACGCTGATGTCAA-3′; and reverse, 5′-GCAACACTTTGGCAGTCTCA-3′.

Monocyte binding assay. Confluent HAEC monolayers were cocultured with human monocytic cell line THP-1 stained with Vybrant CFDA-SE vital dye (Invitrogen) as previously described (Valenzuela et al., 2013). After 10 min at 37°C, 5% CO_2 in static conditions, unbound THP-1 cells were washed and the co-cultures were fixed with 4% PFA. Bound CFDA-SE^+ THP1 cells were imaged with an inverse fluorescent microscope (Carl Zeiss). Bound cells were counted in 10 fields per condition using ImageJ software (National Institutes of Health).

Statistics. Appropriate Student's *t* test was used to determine significant differences between two groups using Prism software (GraphPad Software). $P < 0.05$ was considered significant and reported to the graphs. Data are represented as mean ± SEM.

Study approvals. The IRB evaluated the study and determined that the specimens used for isolation of HAECs qualified for exception number 4. The study of microscopic slides of coronary arteries was approved by the IRB at UCLA (IRB#12-000608). Animal experiments were conducted in accordance with UCLA Department of Laboratory Animal Medicine's Animal Research Committee guidelines (#2005-113-23).

Online supplemental material. Table S1 includes primer sequences for human cDNA amplification. Online supplemental material is available at http://www.jem.org/cgi/content/full/jem.20150603/DC1.

ACKNOWLEDGMENTS

The authors wish to thank Michelle Steel, Benjamin Emert, and Longsheng Hong for valuable technical assistance; Dr Geraldine Weinmaster for providing the plasmid-encoding ZEDN1 construct; Dr. Freddy Radtke for the Notch1 floxed mice; the contribution of the Tissue Procurement Core Laboratory Shared Resource at UCLA; and the UCLA Vector Core supported by CURE/P30 DK041301 for the cloning and virus production. The Illumina Beadchip hybridizations were performed at UCLA Neurosciences Genomics Core.

This study was supported by funds from the American Heart Association #14POST20380819 (to A. Briot) and #13BGIA17110079 (to C. Hong); American Diabetes Association grant 1-14-JF-33 (to C. Hong), Ruth L. Kirschstein National Research Service Award T32HL69766 and K99HL121172 (to M. Civelek), HL28481 (to A.J. Lusis) and HL30568 (to M.L. Iruela-Arispe, A.J. Lusis, J.A. Berliner, A.M. Fogelman, P. Tontonoz, and M. Navab), the Piansky Family Endowment (to M.C. Fishbein), and a grant from the National Institutes of Health (R01 HL085618 to M.L. Iruela-Arispe). S.D. Lee was supported by a postdoctoral fellowship from the Canadian Institutes of Health Research.

A.M. Fogelman and M. Navab are principal investigators in Bruin Pharma, and A.M. Fogelman is an officer in Bruin Pharma. All other authors declare no competing financial interests.

Submitted: 2 April 2015
Accepted: 21 September 2015

REFERENCES

Aoyama, T., K. Takeshita, R. Kikuchi, K. Yamamoto, X.W. Cheng, J.K. Liao, and T. Murohara. 2009. γ-Secretase inhibitor reduces diet-induced atherosclerosis in apolipoprotein E-deficient mice. *Biochem. Biophys. Res. Commun.* 383:216–221. http://dx.doi.org/10.1016/j.bbrc.2009.03.154

Bradley, M.N., C. Hong, M. Chen, S.B. Joseph, D.C. Wilpitz, X. Wang, A.J. Lusis, A. Collins, W.A. Hseuh, J.L. Collins, et al. 2007. Ligand activation of LXRβ reverses atherosclerosis and cellular cholesterol overload in mice lacking LXRα and apoE. *J. Clin. Invest.* 117:2337–2346. http://dx.doi.org/10.1172/JCI31909

Brånén, L., L. Hovgaard, M. Nitulescu, E. Bengtsson, J. Nilsson, and S. Jovinge. 2004. Inhibition of tumor necrosis factor-alpha reduces atherosclerosis in apolipoprotein E knockout mice. *Arterioscler. Thromb. Vasc. Biol.* 24:2137–2142. http://dx.doi.org/10.1161/01.ATV.0000143933.20616.1b

Briot, A., A. Jaroszewicz, C.M. Warren, J. Lu, M. Touma, C. Rudat, J.J. Hofmann, R. Airik, G. Weinmaster, K. Lyons, et al. 2014. Repression of Sox9 by Jag1 is continuously required to suppress the default chondrogenic fate of vascular smooth muscle cells. *Dev. Cell.* 31:707–721. http://dx.doi.org/10.1016/j.devcel.2014.11.023

Calkin, A.C., S.D. Lee, J. Kim, C.M. Van Stijn, X.H. Wu, A.J. Lusis, C. Hong, R.I. Tangirala, and P. Tontonoz. 2014. Transgenic expression of dominant-active IDOL in liver causes diet-induced hypercholesterolemia and atherosclerosis in mice. *Circ. Res.* 115:442–449. http://dx.doi.org/10.1161/CIRCRESAHA.115.304440

Chen, C., and H. Okayama. 1987. High-efficiency transformation of mammalian cells by plasmid DNA. *Mol. Cell. Biol.* 7:2745–2752. http://dx.doi.org/10.1128/MCB.7.8.2745

De Strooper, B. 2003. Aph-1, Pen-2, and Nicastrin with Presenilin generate an active γ-Secretase complex. *Neuron.* 38:9–12. http://dx.doi.org/10.1016/S0896-6273(03)00205-8

Emert, B., Y. Hasin-Brumshtein, J.R. Springstead, L. Vakili, J.A. Berliner, and A.J. Lusis. 2014. HDL inhibits the effects of oxidized phospholipids on endothelial cell gene expression via multiple mechanisms. *J. Lipid Res.* 55:1678–1692. http://dx.doi.org/10.1194/jlr.M047738

Erbilgin, A., M. Civelek, C.E. Romanoski, C. Pan, R. Hagopian, J.A. Berliner, and A.J. Lusis. 2013a. Identification of CAD candidate genes in GWAS loci and their expression in vascular cells. *J. Lipid Res.* 54:1894–1905. http://dx.doi.org/10.1194/jlr.M037085

Erbilgin, A., N. Siemers, P. Kayne, W.P. Yang, J. Berliner, and A.J. Lusis. 2013b. Gene expression analyses of mouse aortic endothelium in response to atherogenic stimuli. *Arterioscler. Thromb. Vasc. Biol.* 33:2509–2517. http://dx.doi.org/10.1161/ATVBAHA.113.301989

Fukuda, D., E. Aikawa, F.K. Swirski, T.I. Novobrantseva, V. Kotelianski, C.Z. Gorgun, A. Chudnovskiy, H. Yamazaki, K. Croce, R. Weissleder, et al. 2012. Notch ligand Delta-like 4 blockade attenuates atherosclerosis and metabolic disorders. *Proc. Natl. Acad. Sci. USA.* 109:E1868–E1877. http://dx.doi.org/10.1073/pnas.1116889109

Gargalovic, P.S., M. Imura, B. Zhang, N.M. Gharavi, M.J. Clark, J. Pagnon, W.P. Yang, A. He, A. Truong, S. Patel, et al. 2006. Identification of inflammatory gene modules based on variations of human endothelial cell responses to oxidized lipids. *Proc. Natl. Acad. Sci. USA.* 103:12741–12746. http://dx.doi.org/10.1073/pnas.0605457103

Gautier, L., L. Cope, B.M. Bolstad, and R.A. Irizarry. 2004. affy—analysis of Affymetrix GeneChip data at the probe level. *Bioinformatics.* 20:307–315. http://dx.doi.org/10.1093/bioinformatics/btg405

Ghosh, S., J. Vivar, C.P. Nelson, C. Willenborg, A.V. Segrè, V.P. Mäkinen, M. Nikpay, J. Erdmann, S. Blankenberg, C. O'Donnell, et al. 2015. Systems genetics analysis of genome-wide association study reveals novel associations between key biological processes and coronary artery disease. *Arterioscler. Thromb. Vasc. Biol.* 35:1712–1722. http://dx.doi.org/10.1161/ATVBAHA.115.305513

Gridley, T. 2010. Notch signaling in the vasculature. *Curr. Top. Dev. Biol.* 92:277–309. http://dx.doi.org/10.1016/S0070-2153(10)92009-7

Guo, D., J.D. Dunbar, C.H. Yang, L.M. Pfeffer, and D.B. Donner. 1998. Induction of Jak/STAT signaling by activation of the type 1 TNF receptor. *J. Immunol.* 160:2742–2750.

Guruharsha, K.G., M.W. Kankel, and S. Artavanis-Tsakonas. 2012. The Notch signalling system: recent insights into the complexity of a conserved pathway. *Nat. Rev. Genet.* 13:654–666. http://dx.doi.org/10.1038/nrg3272

Hellström, M., L.K. Phng, J.J. Hofmann, E. Wallgard, L. Coultas, P. Lindblom, J. Alva, A.K. Nilsson, L. Karlsson, N. Gaiano, et al. 2007. Dll4 signalling through Notch1 regulates formation of tip cells during angiogenesis. *Nature.* 445:776–780. http://dx.doi.org/10.1038/nature05571

Hofmann, J.J., A. Briot, J. Enciso, A.C. Zovein, S. Ren, Z.W. Zhang, F. Radtke, M. Simons, Y. Wang, and M.L. Iruela-Arispe. 2012. Endothelial deletion of murine Jag1 leads to valve calcification and congenital heart defects associated with Alagille syndrome. *Development.* 139:4449–4460. http://dx.doi.org/10.1242/dev.084871

Hossain, G.S., J.V. van Thienen, G.H. Werstuck, J. Zhou, S.K. Sood, J.G. Dickhout, A.B. de Koning, D. Tang, D. Wu, E. Falk, et al. 2003. TDAG51 is induced by homocysteine, promotes detachment-mediated programmed cell death, and contributes to the development of atherosclerosis in

hyperhomocysteinemia. *J. Biol. Chem.* 278:30317–30327. http://dx.doi.org/10.1074/jbc.M212897200

Kang, H.M., J.H. Sul, S.K. Service, N.A. Zaitlen, S.Y. Kong, N.B. Freimer, C. Sabatti, and E. Eskin. 2010. Variance component model to account for sample structure in genome-wide association studies. *Nat. Genet.* 42:348–354. http://dx.doi.org/10.1038/ng.548

Lee, S., K.G. Birukov, C.E. Romanoski, J.R. Springstead, A.J. Lusis, and J.A. Berliner. 2012. Role of phospholipid oxidation products in atherosclerosis. *Circ. Res.* 111:778–799. http://dx.doi.org/10.1161/CIRCRESAHA.111.256859

Leitinger, N., T.R. Tyner, L. Oslund, C. Rizza, G. Subbanagounder, H. Lee, P.T. Shih, N. Mackman, G. Tigyi, M.C. Territo, et al. 1999. Structurally similar oxidized phospholipids differentially regulate endothelial binding of monocytes and neutrophils. *Proc. Natl. Acad. Sci. USA.* 96:12010–12015. http://dx.doi.org/10.1073/pnas.96.21.12010

Li, X., L. Tu, P.G. Murphy, T. Kadono, D.A. Steeber, and T.F. Tedder. 2001. CHST1 and CHST2 sulfotransferase expression by vascular endothelial cells regulates shear-resistant leukocyte rolling via L-selectin. *J. Leukoc. Biol.* 69:565–574.

Lichtman, A.H., C.J. Binder, S. Tsimikas, and J.L. Witztum. 2013. Adaptive immunity in atherogenesis: new insights and therapeutic approaches. *J. Clin. Invest.* 123:27–36. http://dx.doi.org/10.1172/JCI63108

Liu, Z.J., Y. Tan, G.W. Beecham, D.M. Seo, R. Tian, Y. Li, R.I. Vazquez-Padron, M. Pericak-Vance, J.M. Vance, P.J. Goldschmidt-Clermont, et al. 2012. Notch activation induces endothelial cell senescence and pro-inflammatory response: implication of Notch signaling in atherosclerosis. *Atherosclerosis.* 225:296–303. http://dx.doi.org/10.1016/j.atherosclerosis.2012.04.010

Lobov, I.B., R.A. Renard, N. Papadopoulos, N.W. Gale, G. Thurston, G.D. Yancopoulos, and S.J. Wiegand. 2007. Delta-like ligand 4 (Dll4) is induced by VEGF as a negative regulator of angiogenic sprouting. *Proc. Natl. Acad. Sci. USA.* 104:3219–3224. http://dx.doi.org/10.1073/pnas.0611206104

MacKenzie, F., P. Duriez, F. Wong, M. Noseda, and A. Karsan. 2004. Notch4 inhibits endothelial apoptosis via RBP-Jκ-dependent and -independent pathways. *J. Biol. Chem.* 279:11657–11663. http://dx.doi.org/10.1074/jbc.M312102200

Madisen, L., T.A. Zwingman, S.M. Sunkin, S.W. Oh, H.A. Zariwala, H. Gu, L.L. Ng, R.D. Palmiter, M.J. Hawrylycz, A.R. Jones, et al. 2010. A robust and high-throughput Cre reporting and characterization system for the whole mouse brain. *Nat. Neurosci.* 13:133–140. http://dx.doi.org/10.1038/nn.2467

Mäkinen, V.P., M. Civelek, Q. Meng, B. Zhang, J. Zhu, C. Levian, T. Huan, A.V. Segrè, S. Ghosh, J. Vivar, et al. Coronary ARtery DIsease Genome-Wide Replication And Meta-Analysis (CARDIoGRAM) Consortium. 2014. Integrative genomics reveals novel molecular pathways and gene networks for coronary artery disease. *PLoS Genet.* 10:e1004502. http://dx.doi.org/10.1371/journal.pgen.1004502

Mineo, C., and P.W. Shaul. 2013. Regulation of signal transduction by HDL. *J. Lipid Res.* 54:2315–2324. http://dx.doi.org/10.1194/jlr.R039479

Naldini, L., U. Blömer, F.H. Gage, D. Trono, and I.M. Verma. 1996. Efficient transfer, integration, and sustained long-term expression of the transgene in adult rat brains injected with a lentiviral vector. *Proc. Natl. Acad. Sci. USA.* 93:11382–11388. http://dx.doi.org/10.1073/pnas.93.21.11382

Navab, M., G.P. Hough, L.W. Stevenson, D.C. Drinkwater, H. Laks, and A.M. Fogelman. 1988. Monocyte migration into the subendothelial space of a coculture of adult human aortic endothelial and smooth muscle cells. *J. Clin. Invest.* 82:1853–1863. http://dx.doi.org/10.1172/JCI113802

Nus, M., D. MacGrogan, B. Martínez-Poveda, Y. Benito, J.C. Casanova, F. Fernández-Avilés, J. Bermejo, and J.L. de la Pompa. 2011. Diet-induced aortic valve disease in mice haploinsufficient for the Notch pathway effector RBPJK/CSL. *Arterioscler. Thromb. Vasc. Biol.* 31:1580–1588. http://dx.doi.org/10.1161/ATVBAHA.111.227561

Oskolkova, O.V., T. Afonyushkin, B. Preinerstorfer, W. Bicker, E. von Schlieffen, E. Hainzl, S. Demyanets, G. Schabbauer, W. Lindner, A.D. Tselepis, et al. 2010. Oxidized phospholipids are more potent antagonists of lipopolysaccharide than inducers of inflammation. *J. Immunol.* 185:7706–7712. http://dx.doi.org/10.4049/jimmunol.0903594

Qamar, A., and D.J. Rader. 2012. Effect of interleukin 1β inhibition in cardiovascular disease. *Curr. Opin. Lipidol.* 23:548–553. http://dx.doi.org/10.1097/MOL.0b013e328359b0a6

Quillard, T., S. Coupel, F. Coulon, J. Fitau, M. Chatelais, M.C. Cuturi, E. Chiffoleau, and B. Charreau. 2008. Impaired Notch4 activity elicits endothelial cell activation and apoptosis: implication for transplant arteriosclerosis. *Arterioscler. Thromb. Vasc. Biol.* 28:2258–2265. http://dx.doi.org/10.1161/ATVBAHA.108.174995

Quillard, T., J. Devallière, S. Coupel, and B. Charreau. 2010. Inflammation dysregulates Notch signaling in endothelial cells: implication of Notch2 and Notch4 to endothelial dysfunction. *Biochem. Pharmacol.* 80:2032–2041. http://dx.doi.org/10.1016/j.bcp.2010.07.010

Radtke, F., A. Wilson, G. Stark, M. Bauer, J. van Meerwijk, H.R. MacDonald, and M. Aguet. 1999. Deficient T cell fate specification in mice with an induced inactivation of Notch1. *Immunity.* 10:547–558. http://dx.doi.org/10.1016/S1074-7613(00)80054-0

Ramasamy, S.K., A.P. Kusumbe, L. Wang, and R.H. Adams. 2014. Endothelial Notch activity promotes angiogenesis and osteogenesis in bone. *Nature.* 507:376–380. http://dx.doi.org/10.1038/nature13146

Ritchie, M.E., J. Silver, A. Oshlack, M. Holmes, D. Diyagama, A. Holloway, and G.K. Smyth. 2007. A comparison of background correction methods for two-colour microarrays. *Bioinformatics.* 23:2700–2707. http://dx.doi.org/10.1093/bioinformatics/btm412

Riwanto, M., and U. Landmesser. 2013. High density lipoproteins and endothelial functions: mechanistic insights and alterations in cardiovascular disease. *J. Lipid Res.* 54:3227–3243. http://dx.doi.org/10.1194/jlr.R037762

Rizzo, P., L. Miele, and R. Ferrari. 2013. The Notch pathway: a crossroad between the life and death of the endothelium. *Eur. Heart J.* 34:2504–2509. http://dx.doi.org/10.1093/eurheartj/ehs141

Romanoski, C.E., S. Lee, M.J. Kim, L. Ingram-Drake, C.L. Plaisier, R. Yordanova, C. Tilford, B. Guan, A. He, P.S. Gargalovic, et al. 2010. Systems genetics analysis of gene-by-environment interactions in human cells. *Am. J. Hum. Genet.* 86:399–410. http://dx.doi.org/10.1016/j.ajhg.2010.02.002

Romanoski, C.E., N. Che, F. Yin, N. Mai, D. Pouldar, M. Civelek, C. Pan, S. Lee, L. Vakili, W.P. Yang, et al. 2011. Network for activation of human endothelial cells by oxidized phospholipids: a critical role of heme oxygenase 1. *Circ. Res.* 109:e27–e41. http://dx.doi.org/10.1161/CIRCRESAHA.111.241869

Rostama, B., S.M. Peterson, C.P. Vary, and L. Liaw. 2014. Notch signal integration in the vasculature during remodeling. *Vascul. Pharmacol.* 63:97–104. http://dx.doi.org/10.1016/j.vph.2014.10.003

Rye, K.A., and P.J. Barter. 2014. Cardioprotective functions of HDLs. *J. Lipid Res.* 55:168–179. http://dx.doi.org/10.1194/jlr.R039297

Sakoda, T., K. Kaibuchi, K. Kishi, S. Kishida, K. Doi, M. Hoshino, S. Hattori, and Y. Takai. 1992. smg/rap1/Krev-1 p21s inhibit the signal pathway to the c-fos promoter/enhancer from c-Ki-ras p21 but not from c-raf-1 kinase in NIH3T3 cells. *Oncogene.* 7:1705–1711.

Sakoda, T., N. Kasahara, Y. Hamamori, and L. Kedes. 1999. A high-titer lentiviral production system mediates efficient transduction of differentiated cells including beating cardiac myocytes. *J. Mol. Cell. Cardiol.* 31:2037–2047. http://dx.doi.org/10.1006/jmcc.1999.1035

Schober, A., M. Nazari-Jahantigh, Y. Wei, K. Bidzhekov, F. Gremse, J. Grommes, R.T. Megens, K. Heyll, H. Noels, M. Hristov, et al. 2014. MicroRNA-126-5p promotes endothelial proliferation and limits atherosclerosis by suppressing Dlk1. *Nat. Med.* 20:368–376. http://dx.doi.org/10.1038/nm.3487

Shawber, C., D. Nofziger, J.J. Hsieh, C. Lindsell, O. Bögler, D. Hayward, and G. Weinmaster. 1996. Notch signaling inhibits muscle cell differentiation through a CBF1-independent pathway. *Development.* 122:3765–3773.

Shih, D.M., L. Gu, Y.R. Xia, M. Navab, W.F. Li, S. Hama, L.W. Castellani, C.E. Furlong, L.G. Costa, A.M. Fogelman, and A.J. Lusis. 1998. Mice lacking serum paraoxonase are susceptible to organophosphate toxicity and atherosclerosis. *Nature.* 394:284–287. http://dx.doi.org/10.1038/28406

Siti, H.N., Y. Kamisah, and J. Kamsiah. 2015. The role of oxidative stress, antioxidants and vascular inflammation in cardiovascular disease (a review). *Vascul. Pharmacol.* 71:40–56. http://dx.doi.org/10.1016/j.vph.2015.03.005

Subbanagounder, G., N. Leitinger, D.C. Schwenke, J.W. Wong, H. Lee, C. Rizza, A.D. Watson, K.F. Faull, A.M. Fogelman, and J.A. Berliner. 2000. Determinants of bioactivity of oxidized phospholipids. Specific oxidized fatty acyl groups at the sn-2 position. *Arterioscler. Thromb. Vasc. Biol.* 20:2248–2254. http://dx.doi.org/10.1161/01.ATV.20.10.2248

Suchting, S., C. Freitas, F. le Noble, R. Benedito, C. Bréant, A. Duarte, and A. Eichmann. 2007. The Notch ligand Delta-like 4 negatively regulates endothelial tip cell formation and vessel branching. *Proc. Natl. Acad. Sci. USA.* 104:3225–3230. http://dx.doi.org/10.1073/pnas.0611177104

Tangirala, R.K., E.M. Rubin, and W. Palinski. 1995. Quantitation of atherosclerosis in murine models: correlation between lesions in the aortic origin and in the entire aorta, and differences in the extent of lesions between sexes in LDL receptor-deficient and apolipoprotein E-deficient mice. *J. Lipid Res.* 36:2320–2328.

Tangirala, R.K., K. Tsukamoto, S.H. Chun, D. Usher, E. Puré, and D.J. Rader. 1999. Regression of atherosclerosis induced by liver-directed gene transfer of apolipoprotein A-I in mice. *Circulation.* 100:1816–1822. http://dx.doi.org/10.1161/01.CIR.100.17.1816

Teslovich, T.M., K. Musunuru, A.V. Smith, A.C. Edmondson, I.M. Stylianou, M. Koseki, J.P. Pirruccello, S. Ripatti, D.I. Chasman, C.J. Willer, et al. 2010. Biological, clinical and population relevance of 95 loci for blood lipids. *Nature.* 466:707–713. http://dx.doi.org/10.1038/nature09270

Theodoris, C.V., M. Li, M.P. White, L. Liu, D. He, K.S. Pollard, B.G. Bruneau, and D. Srivastava. 2015. Human disease modeling reveals integrated transcriptional and epigenetic mechanisms of NOTCH1 haploinsufficiency. *Cell.* 160:1072–1086. http://dx.doi.org/10.1016/j.cell.2015.02.035

Valenzuela, N.M., A. Mulder, and E.F. Reed. 2013. HLA class I antibodies trigger increased adherence of monocytes to endothelial cells by eliciting an increase in endothelial P-selectin and, depending on subclass, by engaging FcγRs. *J. Immunol.* 190:6635–6650. http://dx.doi.org/10.4049/jimmunol.1201434

Walshe, T.E., P. Connell, L. Cryan, G. Ferguson, T. Gardiner, D. Morrow, E.M. Redmond, C. O'Brien, and P.A. Cahill. 2011. Microvascular retinal endothelial and pericyte cell apoptosis in vitro: role of hedgehog and Notch signaling. *Invest. Ophthalmol. Vis. Sci.* 52:4472–4483. http://dx.doi.org/10.1167/iovs.10-7061

Wang, L., H. Zhang, S. Rodriguez, L. Cao, J. Parish, C. Mumaw, A. Zollman, M.M. Kamoka, J. Mu, D.Z. Chen, et al. 2014. Notch-dependent repression of miR-155 in the bone marrow niche regulates hematopoiesis in an NF-κB-dependent manner. *Cell Stem Cell.* 15:51–65. http://dx.doi.org/10.1016/j.stem.2014.04.021

Wang, Y., M. Nakayama, M.E. Pitulescu, T.S. Schmidt, M.L. Bochenek, A. Sakakibara, S. Adams, A. Davy, U. Deutsch, U. Lüthi, et al. 2010. Ephrin-B2 controls VEGF-induced angiogenesis and lymphangiogenesis. *Nature.* 465:483–486. http://dx.doi.org/10.1038/nature09002

Watson, A.D., N. Leitinger, M. Navab, K.F. Faull, S. Hörkkö, J.L. Witztum, W. Palinski, D. Schwenke, R.G. Salomon, W. Sha, et al. 1997. Structural identification by mass spectrometry of oxidized phospholipids in minimally oxidized low density lipoprotein that induce monocyte/endothelial interactions and evidence for their presence in vivo. *J. Biol. Chem.* 272:13597–13607. http://dx.doi.org/10.1074/jbc.272.21.13597

Willer, C.J., E.M. Schmidt, S. Sengupta, G.M. Peloso, S. Gustafsson, S. Kanoni, A. Ganna, J. Chen, M.L. Buchkovich, S. Mora, et al. Global Lipids Genetics Consortium. 2013. Discovery and refinement of loci associated with lipid levels. *Nat. Genet.* 45:1274–1283. http://dx.doi.org/10.1038/ng.2797

Zhou, Z., P. Subramanian, G. Sevilmis, B. Globke, O. Soehnlein, E. Karshovska, R. Megens, K. Heyll, J. Chun, J.S. Saulnier-Blache, et al. 2011. Lipoprotein-derived lysophosphatidic acid promotes atherosclerosis by releasing CXCL1 from the endothelium. *Cell Metab.* 13:592–600. http://dx.doi.org/10.1016/j.cmet.2011.02.016

SUPPLEMENTAL MATERIAL

Briot et al., http://www.jem.org/cgi/content/full/jem.20150603/DC1

Table S1. **Primer sequences for cDNA amplification**

Target cDNA	Forward sequence (5′–3′)	Reverse sequence (5′–3′)
HPRT	GCCCTGGCGTCGTGATTAGT	AGCAAGACGTTCAGTCCTGTC
NOTCH1	ACTGTGAGGACCTGGTGGAC	TTGTAGGTGTTGGGGAGGTC
NOTCH2	TGTGACATAGCAGCCTCCAG	CAGGGGGCACTGACAGTAAT
NOTCH3	GCATAGGCCAGTTCACCTGT	AATGTCCACCTCGCAATAGG
NOTCH4	CTAGGGGCTCTTCTCGTCCT	CAACTTCTGCCTTTGGCTTC
JAG1	GACTCATCAGCCGTGTCTCA	TGGGGAACACTCACACTCAA
HES1	TCAACACGACACCGGATAAA	TCAGCTGGCTCAGACTTTCA
HEYL	AGATGCAAGCCAGGAAGAAA	TCTCGACGCCGTTTCTCTAT
IL8	AAGAAACCACCGGAAGGAAC	ACTCCTTGGCAAAACTGCAC
CXCL1/GROα	AGCTTGCCTCAATCCTGCAT	TCCTCCTCCCTTCTGGTCAG
TDAG51	CTCTCATCCTCACTCGCACC	CGTCCCACTTCCTCAAGTCC
HO-1	GGCAGAGAATGCTGAGTTCAT	ATAGATGTGGTACAGGGAGGC
SELE	AAGGCTTCATGTTGCAGGGA	ATTCATGTAGCCTCGCTCGG
CHST1	GACTTTCTCCCCAGCTGCAT	CTGCTTCTCCAAGGGGTGAG